


# Eliminating malaria transmission requires targeting immature and mature gametocytes through lipoidal uptake of antimalarials

Received: 28 March 2024

Accepted: 1 November 2024

Published online: 15 November 2024

 Check for updates

Mariska Naude<sup>1,2</sup>, Ashleigh van Heerden<sup>1,2</sup>, Janette Reader<sup>1,2</sup>, Mariëtte van der Watt<sup>2</sup>, Jandeli Niemand<sup>1,2</sup>, Dorè Joubert<sup>1</sup>, Giulia Siciliano<sup>3</sup>, Pietro Alano<sup>3</sup>, Mathew Njoroge<sup>4</sup>, Kelly Chibale<sup>4,5</sup>, Esperanza Herreros<sup>6</sup>, Didier Leroy<sup>6</sup> & Lyn-Marié Birkholtz<sup>1,2,7</sup> 

Novel antimalarial compounds targeting both the pathogenic and transmissible stages of the human malaria parasite, *Plasmodium falciparum*, would greatly benefit malaria elimination strategies. However, most compounds affecting asexual blood stage parasites show severely reduced activity against gametocytes. The impact of this activity loss on a compound's transmission-blocking activity is unclear. Here, we report the systematic evaluation of the activity loss against gametocytes and investigate the confounding factors contributing to this. A threshold for acceptable activity loss between asexual blood stage parasites and gametocytes was defined, with near-equipotent compounds required to prevent continued gametocyte maturation and onward transmission. Target abundance is not predictive of gametocytocidal activity, but instead, lipoidal uptake is the main barrier of dual activity and is influenced by distinct physicochemical properties. This study provides guidelines for the required profiles of potential dual-active antimalarial agents and facilitates the development of effective transmission-blocking compounds.

Malaria remains a global health burden, with malaria cases and deaths concerning on the rise in the aftermath of the COVID-19 pandemic<sup>1</sup>. The continued emergence of parasite resistance to current antimalarials drives the need for new compounds that should target novel, essential biology in *Plasmodium falciparum*, with the ability to target multiple stages of the parasites seen as an enticing added advantage. Transmission-blocking activity is particularly desirable as it will prevent the spread of resistance in the parasite population once it has

developed<sup>2</sup>. This would require targeting mature gametocytes in the human host to prevent transmission to the mosquito<sup>2</sup>. Gametocytes differentiate from a subset ( $\leq 10\%$ )<sup>3</sup> of the proliferating and pathogenic asexual blood stage (ABS) parasites and mature in a prolonged ~12-day process in *P. falciparum*.

Most antimalarial compounds are only active against ABS parasites without pronounced activity against mature gametocytes<sup>2,4,5</sup>, with some also not retaining activity against immature gametocytes (e.g.

<sup>1</sup>Department of Biochemistry, Genetics and Microbiology, University of Pretoria, Hatfield, Pretoria 0028, South Africa. <sup>2</sup>Institute for Sustainable Malaria Control, University of Pretoria, Hatfield, Pretoria 0028, South Africa. <sup>3</sup>Dipartimento di Malattie Infettive, Istituto Superiore di Sanità, viale Regina Elena 299, 00161 Rome, Italy. <sup>4</sup>Drug Discovery and Development Centre (H3D), University of Cape Town, Rondebosch, Cape Town 7701, South Africa. <sup>5</sup>South African Medical Research Council Drug Discovery and Development Research Unit, Department of Chemistry and Institute of Infectious Disease and Molecular Medicine, University of Cape Town, Rondebosch, Cape Town 7701, South Africa. <sup>6</sup>Medicines for Malaria Venture, Geneva, Switzerland. <sup>7</sup>Department of Biochemistry, Stellenbosch University, Matieland, Stellenbosch 7602, South Africa. ✉e-mail: [lbirkholtz@up.ac.za](mailto:lbirkholtz@up.ac.za)

pyrimethamine and atovaquone<sup>4</sup>). The development priority remains for combinations of ‘dual-active’ compounds with ‘equipotent’ activity against both ABS parasites and gametocytes. However, when additional gametocytocidal activity is present in dual-active compounds, it is usually associated with reduced activity against gametocytes compared to the activity against ABS parasites. Direct comparison of compounds’ activities against the parasite’s different stages has been complicated due to intrinsic assay differences that measure the activity of a compound against ABS parasites (cell proliferation assays), gametocytes (cell viability assays<sup>4,6,7</sup>), and gametes (functional cell differentiation<sup>8</sup>). Importantly, the threshold at which this loss in activity would be acceptable to still ensure efficacy in a therapeutic context has not been defined. Indeed, we also lack clarity on the impact such a loss in activity would have on the transmission-blocking activity of dual-active antimalarial candidates. This information is crucial to accurately classify and develop a candidate according to its target candidate profile.

A systematic evaluation of the underlying reasons for the loss of activity of compounds between ABS parasites and immature and mature gametocytes has not been performed, and this hampers efforts at optimizing antimalarial candidates for additional transmission-blocking activity. Target availability, compound uptake, and efflux can all influence an antimalarial compound’s activity. Indeed, the differential biology of the parasite’s life cycle stages<sup>9,10</sup> can result in differences in drug target abundance or uptake mechanisms between ABS parasites and mature gametocytes<sup>2,4,11</sup>, aspects that must be defined and considered to ensure transmission-blocking activity.

Here, we simultaneously evaluated the activity of antiplasmodial compounds and lead clinical development candidates on multiple stages of *P. falciparum* parasites to provide a classification model for therapeutically relevant dual activity on ABS parasites and gametocytes. We investigated the reasons for the differential activities of compounds, including the influence of different assay platforms, the differences in target availability between the stages, and the

physicochemical properties mediating differentiating uptake into the different stages. Our data point to an acceptable threshold for dual activity where only compounds with <10-fold loss in activity between ABS parasites and gametocytes would realistically have transmission-blocking potential. Critically, we show that immature gametocytes must be cleared to prevent seeding of gametocyte maturation. We show that the uptake of compounds into ABS parasites and gametocytes is a primary barrier to equipotency in cases where the drug target is available in both stages. This work provides a comprehensive framework of the required characteristics for potential dual-active antiplasmodial agents.

## Results

### Classification of the stage-specific activity of compounds against *P. falciparum* parasites

We first aimed to obtain a landscape of the activity profiles of compounds evaluated in vitro against different stages of *P. falciparum* to understand the extent of the activity loss between these stages, as reported previously. We evaluated published IC<sub>50</sub> data from 2013 compounds (Supplementary Fig. S1, Supplementary Data S1). K-means clustering of 118 compounds from this dataset for which IC<sub>50</sub> values were available across all stages (ABS parasites, immature, late-stage IV/V, and mature stage V gametocytes) allowed quantification of the amplitude of activity loss across the different stages. As expected, compounds such as atovaquone, the antifolates (pyrimethamine and P218), and tetracycline antibiotics have a significant loss in activity in gametocytes ( $p=0.0001$ , Kruskal–Wallis test), including immature gametocytes (7–19-fold activity loss, clusters 1 and 8,  $p=0.0001$ , Kruskal–Wallis test, Fig. 1). A significant 3–12-fold loss in activity towards immature gametocytes is retained by the 4- and 8-aminoquinolines (e.g., amodiaquine) and also by the diamine pentamidine and antifungal cycloheximide (clusters 3 and 4,  $p=0.02$ , and  $p=0.0001$ , respectively, Kruskal–Wallis test, Fig. 1). This translates to a loss in activity towards mature gametocytes

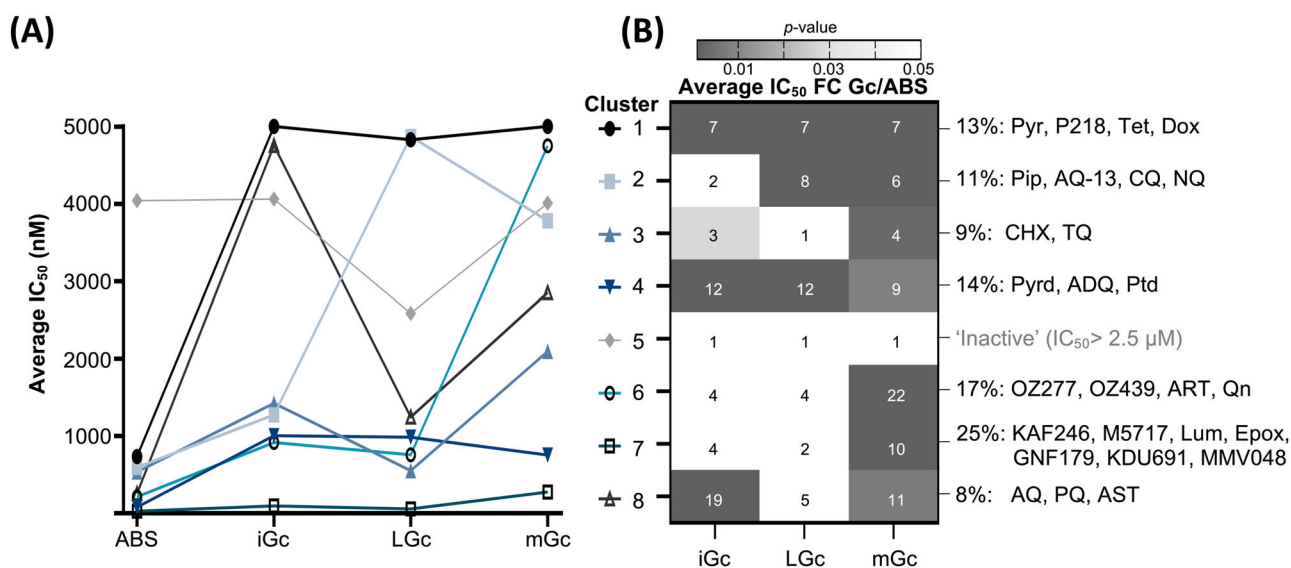


**Fig. 1 | Differential activity profiles of antimalarial compounds against multiple stages of *P. falciparum* parasites.** **A** The activities (IC<sub>50</sub>s) of compounds previously evaluated against different life cycle stages of *P. falciparum* (asexual blood stage parasites (ABS); immature gametocytes (iGc); late-stage gametocytes (LGc) and mature gametocytes (mGc)) were obtained from a meta-analysis of previous work as provided in Supplementary Data S1. These activities (IC<sub>50</sub>s values) were subsequently K-means clustered and the average IC<sub>50</sub>s against ABS parasites, iGc, LGc, and mGc determined in each cluster were shown in the line graphs. **B** For each cluster, the fold change (FC) was calculated between the average IC<sub>50</sub>s as determined against ABS parasites and that determined against different gametocyte

stages ( $\text{[avgIC}_{50} \text{ Gc}] / \text{[avgIC}_{50} \text{ ABS}]$ ) are indicated. The significant difference between the average IC<sub>50</sub>s between the different parasite stages was determined with a Kruskal–Wallis test followed by Dunn’s multiple comparison test, with each  $p$ -value adjusted to account for multiple comparisons. The  $p$ -value for each comparison is indicated in a heat scale. The distribution of compounds to each cluster is indicated as a % of the whole next to the heatmap. ADQ amodiaquine, AQ atovaquone, ART artemisinin, AST astemizole, CHX cyclohexidine, CQ chloroquine, Dox doxycycline, Epox epoxomicin, Lum lumefantrine, MMV048 MMV390048, NQ naphthoquinone, Pip piperazine, PQ primaquine, Ptd pentamidine, Pyr pyrimethamine, Pyrd pyronaridine, Qn quinine, Tet tetracycline, TQ tafenoquine.

(clusters 3, 4 and 6,  $p = 0.0003$ ,  $p = 0.0008$  and  $p = 0.0001$ , respectively, Kruskal–Wallis test, Fig. 1). Compounds in cluster 7 still present with a significant activity loss of 4- and 10-fold loss against immature ( $p = 0.005$ , Kruskal–Wallis test) and mature gametocytes ( $p = 0.0001$ , Kruskal–Wallis test), respectively. These contain most of the frontrunner and development candidates, including the PfATP4 inhibitor KAF246 (NITD246)<sup>12</sup>, the elongation factor 2 (Pfef2) inhibitor Cabamiquine (M5717, MMV643121, DDD107498)<sup>13</sup>, GNF179<sup>14,15</sup> targeting protein excretion and phosphatidylinositol 4-kinase (PffPI4K) inhibitors KDU691 (MMV650381)<sup>16</sup> and MMV390048 (MMV048)<sup>17,18</sup>.

While the above provides some systematic meta-analysis and quantification of the differential activities of compounds previously tested against multiple life cycle stages of *P. falciparum*, the data were generated in different laboratories, and variances in assay platforms and conditions (including parasite strains, compound batches, and incubation times) and parasite stage distribution could all confound interpretation of the data. To circumvent this, we evaluated a selected set of 80 compounds (provided by the Medicines for Malaria Venture, MMV.org) in parallel, in assays using the same compound preparation on different stages of the same parasite strain and culture (drug-sensitive PfNF54). We evaluated the inhibition of ABS proliferation with SYBR Green I fluorescence on synchronized ring-stage parasites ( $94.5 \pm 0.8\%$ ) and gametocytocidal activity using the same luciferase reporter line for immature ( $13.0 \pm 0.6\%$  stage I,  $54.3 \pm 3.5\%$  stage II and  $25.0 \pm 3.6\%$  stage III gametocytes) and mature gametocytes ( $7.3 \pm 1.4\%$  stage IV and  $90.0 \pm 1.7\%$  stage V, Supplementary Fig. S2a)<sup>6,9</sup>.

K-means clustering and principle component analyses (PCA) of the IC<sub>50</sub> data for compounds with IC<sub>50</sub> < 5  $\mu$ M, replicate the activity loss of compounds that in essence, only target ABS parasites, including the antifolates (pyrimethamine, P218), the dihydroorotate dehydrogenase (PfDHODH) inhibitor DSM265 (MMV018912)<sup>19</sup> and the cGMP-dependent protein kinase (PfPKG) inhibitor MMV030084 (MMV084)<sup>20</sup> (cluster 6, Fig. 2A, Supplementary Fig. S2b, Supplementary Data S2). We provide data for frontrunner and in-development compounds for which immature and/or mature gametocytocidal IC<sub>50</sub> data had not been reported, including another PfPKG inhibitor ML10 (MMV1793799)<sup>21</sup> and KAF156 (Ganaplacide, MMV000130) targeting protein secretion<sup>15</sup>. While these compounds are unable to directly kill either immature or mature gametocytes in vitro as measured here (Fig. 2A, Supplementary Data S2), KAF156 can reduce the number of mature gametocytes when immature gametocytes are exposed to the drug, and this translates to a >90% reduction in oocyst formation, supporting its transmission-blocking potential<sup>14</sup>. Similarly, the transmission-blocking ability of PfPKG inhibitors is driven by their ability to prevent the initiation of gametogenesis<sup>21</sup>.

Compounds that retain some activity against immature gametocytes (4–11-fold activity loss,  $p = 0.1142$ , Kruskal–Wallis test,  $n = 3$ ) but not against mature gametocytes (up to a 118-fold loss,  $p = 0.0001$ , Kruskal–Wallis test,  $n = 3$ ), include 4-aminoquinolines (chloroquine (CQ) and amodiaquine), amino alcohols, and the endoperoxides<sup>4,6</sup> but also frontrunner antimalarial candidates MMV688533 (MMV533)<sup>22</sup>, MMV674253 (MMV253-AZ412/ZY19489) as V-type ATPase inhibitor<sup>23</sup> and MMV1582617 (MMV617, NVP-INE963)<sup>24</sup> (cluster 1, Fig. 2A). Compounds that would be defined with dual activity still show a significant 7- and 18-fold drop in activity from ABS parasites to immature ( $p = 0.049$ , Kruskal–Wallis test,  $n = 3$ ) and mature gametocytes ( $p = 0.0046$ , Kruskal–Wallis test,  $n = 3$ ), respectively, with average IC<sub>50</sub>s of 15, 97 and 262 nM against ABS, immature and mature gametocytes (cluster 3, Fig. 2A). These include frontrunners M5717 (Cabamiquine)<sup>13</sup>, MMV048<sup>18</sup> and KDU691<sup>16</sup>, the acetyl-CoA synthetase (PfAcAS) inhibitor MMV693183 (MMV183)<sup>25</sup>, and PfATP4 inhibitors KAE609 (Cipargamin, MMV000073)<sup>12</sup>, a related analog MMV1581373 (MMV373), SJ733 (MMV390482)<sup>26</sup> and

MMV1542945 (MMV945, ACT-451840)<sup>27</sup>. M5717 has slightly increased potency against mature (but not immature) gametocytes, supporting the dual-active nature of this frontrunner candidate (Supplementary Data S2). KAE609 (and its analog MMV373) effectively kills both immature and mature gametocytes, albeit with a significant drop in activity from ABS parasites to mature gametocytes ( $p = 0.0084$ , one-way ANOVA,  $F(2, 6) = 12.30$ ,  $n = 3$ ) but with a potency at <30 nM for KAE609 still present.

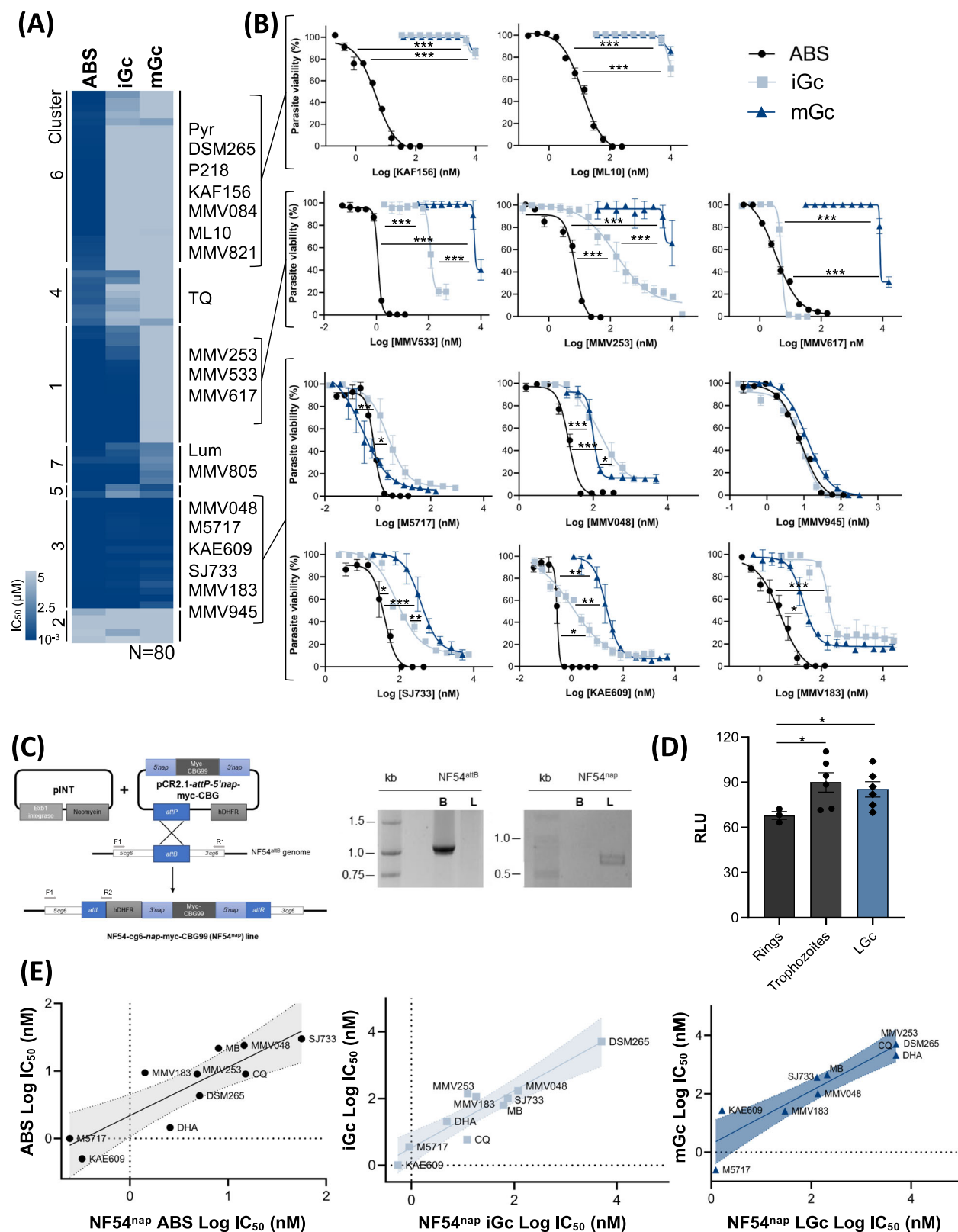
Although the data presented above eliminated much of the confounding factors associated with comparing activities of compounds assayed on different life cycle stages, it still relies on two different assays to measure activity against ABS parasites and gametocytes. To eliminate potential assay interference, we generated a transgenic *P. falciparum* NF54 reporter line that expressed CBG99 luciferase<sup>28</sup> under the control of a constitutive promoter associated with the expression of nuclear assembly protein (*nap*, PF3D7\_091900) in all stages of the parasite's development<sup>9,29</sup>. Genomic integration into the resultant NF54-*cg6-nap-myc-CBG99* line (Fig. 2B) did not affect ABS proliferation rates or gametocytogenesis (Supplementary Fig. S3a, b). Luciferase expression from this line was stable in ABS parasites and gametocytes (Fig. 2C, Supplementary Fig. S3c), with robust viability detected over a wide parasitemia range (Supplementary Fig. S3d).

Three tightly synchronized parasite preparations were obtained from this line and were used to evaluate the activity of a select set of antimalarials ( $95.17 \pm 2.80\%$  ring stage ABS parasites; >93% stage I–III immature gametocytes with ABS parasites removed with both GlcNAc and sorbitol treatment, and late-stage gametocytes at >90% stage IV/V gametocytes; Supplementary Fig. S3e). The IC<sub>50</sub>s of Methylene blue (MB), CQ, and dihydroartemisinin (DHA) are in complete agreement with previous data on all stages evaluated, validating the line and luciferase expression as an indication of viability (Fig. 2D)<sup>5,30</sup>. This translated to a strong positive correlation for the activity of the compounds against ABS parasites (Pearson  $r = 0.77$ , Fig. 2D), immature and late-stage gametocytes (Pearson  $r = 0.99$  and  $r = 0.96$ , respectively, Fig. 2D), indicating that the activity profiles obtained for these antimalarial compounds are not due to assay platform differences.

Together, this data highlights that compounds with apparent activity against ABS parasites, immature, and mature gametocyte stages are not equipotently active, with an average 10- and 18-fold drop in activity between ABS parasites and immature and mature gametocytes, respectively (Fig. 2). As this is not influenced by assay readout, it implies that these parasite stages inherently provide barriers to drug efficacy that are more pronounced than previously perceived.

### Implications of different inhibition profiles on gametocyte stages

Next, we evaluated potential points of concern associated with the activity loss of compounds against immature or mature gametocytes. Previous reports indicated that some antimalarials (DHA, CQ, mefloquine, and sulfadoxine-pyrimethamine<sup>31–33</sup>) targeting ABS parasites, increase commitment of gametocytogenesis, which is a concern if these compounds are not able to kill immature (and mature) gametocytes. Using a transgenic reporter line expressing tdTomato red fluorescence under the *Pfelfla* promoter<sup>34</sup>, we quantified commitment to gametocytogenesis and formation of immature gametocytes when ABS parasites were treated with a select set of frontrunner compounds for 48 h at their respective IC<sub>90</sub> values (Fig. 3A). Under these conditions, commitment to gametocytogenesis was still present with only treatment of ABS parasites with MMV253 and M5717 resulting in a significant reduction in the ability of these parasites to convert to gametocytes ( $p = 0.024$  and  $p = 0.0052$ , respectively, one-way ANOVA,  $F(8, 7.48) = 6.976$ ,  $n = 3$  Fig. 3B). However, at >IC<sub>99</sub> (corresponding to the average human dose exposure concentration, Supplementary Data S3), gametocyte induction was significantly reduced for all compounds evaluated (UT *vs.* DSM265  $p = 0.0001$ , *vs.* CQ  $p = 0.0009$ ,



MMV253  $p = 0.0001$ , MMV533  $p = 0.0008$ , M5717  $p = 0.0009$ , MMV183  $p = 0.0009$ , SJ733  $p = 0.0005$ , MMV048  $p = 0.0007$ , one-way ANOVA,  $F(8, 7.938) = 60.26$ ,  $n = 3$ ).

Compounds will be developed for human dosing in clinical studies based on their activity against ABS parasites and, therefore, the activity of compounds against immature gametocytes had to be evaluated at concentrations relevant to ABS efficacy. Treating immature

gametocytes with M5717, MMV048 and SJ733 at  $IC_{90}$  and  $>10\times IC_{99}$  (corresponding to clinically relevant human doses) was effective at killing these gametocytes when these were present at  $\sim 10\%$  of the ABS parasites' cell numbers, replicating the typical conversion number<sup>3</sup> ( $p = 0.97$ ,  $p = 0.26$  and  $p = 0.18$ , respectively, two-way ANOVA,  $F(2, 42) = 691.0$ ,  $n = 3$ , Fig. 3C). This does not hold for all the other compounds evaluated (MMV183, MMV253, and MM533) where a significant



**Fig. 2 | Parallel evaluation of asexual and gametocytocidal activity of MMV compounds.** The activity ( $IC_{50}$ s) of 80 compounds provided by the MMV were determined in parallel against asexual blood stage (ABS, 95% ring-stages) parasites with SYBR Green I fluorescence after 96 h, and against immature gametocytes (iGc, 80% stage II/III, 13% stage I), and mature gametocytes (mGc, 90% stage V) with luciferase reporter lines after 48 h drug pressures. The data are from  $n = 3$  independent biological repeats, each performed in technical triplicates. **A** K-means clustering of the activities ( $IC_{50}$ s) obtained. **B** Dose-response curves of selected compounds indicate the  $IC_{50}$  shifts between ABS parasites (black), iGc (light blue), and mGc (dark blue). The activities of compounds ( $IC_{50}$ s) were determined from three independent biological repeats ( $n = 3$ ), performed in technical triplicates, mean  $\pm$  S.E., with significance indicated using an unpaired two-tailed Student's  $t$  test. Exact  $p$ -values provided in Supplementary Data S2. **C** Construction of a constitutive luciferase reporter line via Bxb1 *attB-attP* integration of a myc-tagged CBG99 luciferase fusion gene under the control of the 5' nucleosome assembly protein (*nap*) promoter (*prom*) and the 3' regulatory region of the *nap* gene. The

wild-type NF54<sup>attB</sup> and the transgenic line NF54<sup>nap</sup> were PCR screened for the *attB* (**B**) sites which would denote wild-type, unintegrated parasites, whilst the presence of the *attL* (**L**) region will indicate successful integration using primers shown (*attB*: F1 and R1, *attL*: F1 and R2). The expected DNA band sizes were obtained on the gel (*attB*: 1100 bp, *attL*: 701 bp). **D** The bioluminescent signal (RLU) from CBG99 luciferase activity across ABS parasites and gametocytes ( $n = 3$  independent biological experiments for rings;  $n = 6$  independent experiments for trophozoites and LGc, all in technical triplicates, mean  $\pm$  S.E.). Individual data points are indicated in symbols. Statistical evaluation was performed with one-way ANOVA (total DF = 14),  $p = 0.018$  rings *vs.* trophozoites and  $p = 0.019$  rings *vs.* LGc. **E** Correlation of the activities of antimalarial compounds between the constitutive luciferase reporter line and other assay platforms, with 95% confidence bands on each point indicated as ribbons on the regression line. Data from three independent biological repeats ( $n = 3$ ), performed in technical triplicates. CQ Chloroquine, DHA dihydroartemisinin, Lum Lumefantrine, MB Methylene blue, MMV183 MMV693183, MMV253 MMV674253, Pyr Pyrimethamine, TQ Tafenoquine. \* $p < 0.05$ ; \*\* $p < 0.01$ , \*\*\* $p < 0.001$ .

reduction in activity against immature gametocytes was present at these concentrations ( $p = 0.048$ ,  $p = 0.0001$  and  $p = 0.0003$ , respectively, two-way ANOVA,  $F(2, 42) = 691.0$ ,  $n = 3$ ). This was similarly true for the activity of these compounds against late-stage gametocytes at these concentrations (Supplementary Fig. S4b). This raises concerns with compounds with such profiles that will not prevent gametocyte differentiation, with the resultant immature gametocytes not effectively killed.

In the above scenario, immature gametocytes formed when ABS parasites are treated with antimalarial candidates could seed the development of mature gametocytes and sustain transmission. Therefore, we interrogated the compounds' ability to prevent the maturation of gametocytes after immature gametocytes were pulsed on the drug for 48 h. Gametocytemia decreased for all the compounds tested, significantly so for M5717 and MMV533 ( $p = 0.0001$  and  $p = 0.0001$ , respectively, one-way ANOVA,  $F(6, 14) = 20.40$ , Fig. 3A, D). This is similar to the reduction in mature gametocytes after KAF156 treatment of immature gametocytes<sup>14</sup>. The mature stage V gametocytes produced after these drug treatments appeared morphologically somewhat irregular (Supplementary Fig. S4c), with a change in sex ratio, particularly for M5717 that showed a significant decrease in the female-to-male gametocyte ratio ( $p = 0.0244$ , one-way ANOVA,  $F(6, 7) = 9.609$ , Supplementary Fig. S4d). Additionally, gametocytes produced under these conditions showed a similarly decreased ability to produce gamete formation (Fig. 3E), with a significant >80% reduction in gamete formation seen for M5717 ( $p = 0.0001$ , one-way ANOVA,  $F(5, 12) = 36.75$  and  $F(5, 12) = 76.87$ ) and MMV533 (female gametes,  $p = 0.0001$ , one-way ANOVA,  $F(5, 12) = 36.75$ , Fig. 3E). Taken together, compounds that are ineffective at targeting immature gametocytes may also be ineffective at preventing onward parasite transmission to the mosquito.

### Target protein abundance does not correlate to a loss in gametocyte activity profiles

We subsequently investigated potential causes for the differential activities of compounds between ABS parasites and different stages of gametocytes. Stage-specific transcript<sup>9,35–37</sup> and protein<sup>35,38</sup> abundances characterize ABS parasites and various stages of gametocytes. We correlated protein expression profiles of validated and/or putative targets of the compounds across the parasite's life cycle stages with the differential activity profiles of the compounds (Fig. 4, Supplementary Data S4), with the assumption that the activity against ABS parasites and gametocytes is due to the inhibition of the same protein target. A correlation was evident between protein abundance and the compounds' activity only for a few compounds with <10-fold change difference in activity between ABS parasites and both gametocyte stages (Pearson  $r = 0.15$  and  $0.49$  for immature

and mature gametocytes, Supplementary Fig. S5a, c, d). This includes M5717 with <2-fold difference in the abundance of its target PFEF2 between these stages. Similarly, the activity of MMV183 and MMV019721 (MMV721) can be explained by similar abundances of their target PfAcAS (<2-fold difference), as is true for PfPRS (proline-tRNA synthetase) targeted by halofuginone. However, this does not hold for compounds proposed to target PfPheRS (phenylalanine-tRNA synthetase), including BRD3444 and BRD7929, which have a 10-fold loss in activity against immature gametocytes but >1000-fold loss in activity in mature gametocytes even though PfPheRS is equally abundant in these gametocyte stages (cluster 5 for ABS/iGc to cluster 2 for ABS/mGc, Fig. 4). Similarly, SJ733 and KAE609 show a 2–4-fold loss in activity against immature gametocytes and a 12–55-fold loss in efficacy against mature gametocytes, although the abundance of their target (PfATP4) did not decrease. This is also true for PfPKG as the target for ML10 or MMV084. Although quantitative protein data is not available for PfPI4K as it is a membrane-associated protein, transcript levels show only a ~2-fold decreased transcript abundance between ABS parasites and mature gametocytes<sup>9,29</sup>, while PfPI4K inhibitors MMV048 (and related analog MMV642943 (UCT943) and MMV642944) and KDU691 lose ~4–20-fold activity against mature gametocytes. Indeed, there is no overall linear relationship between protein abundance and activity loss for compounds losing >10-fold of their activity in gametocytes implying other factors must be at play to cause the activity loss. Metabolic, biochemical, and essentiality data (Supplementary Data S4) indicate that the function of some of these targets is not essential for gametocyte survival<sup>10,39</sup>. Alternatively, such compounds may not effectively gain access to their cellular site.

### Physicochemical properties contribute to differential profiles of compounds against ABS parasites and gametocytes

To understand if there is a physicochemical space that defines compounds with dual activity, we used cheminformatics and machine learning to deconvolute contributions to compound efficacy. Previously developed machine learning classification models for stage-specific activities of compounds<sup>40</sup> confirmed the specific enrichment in our data for compounds against the different parasite stages, including immature gametocytes (probability >0.7, Supplementary Fig. S6a). We subsequently created various multiclass models (Supplementary Data S5) of which Random Forest (RF) accurately (macro average AUC 0.80, Supplementary Fig. S6b) classified compounds with specific activity profiles based on their physicochemical relatedness<sup>41</sup>. Extraction of the chemical features enriched within these activity profiles identified topological polar surface area (tPSA), molecular weight (MW) and lipophilicity as the most critical chemical features that allow the discrimination of compounds with different activity

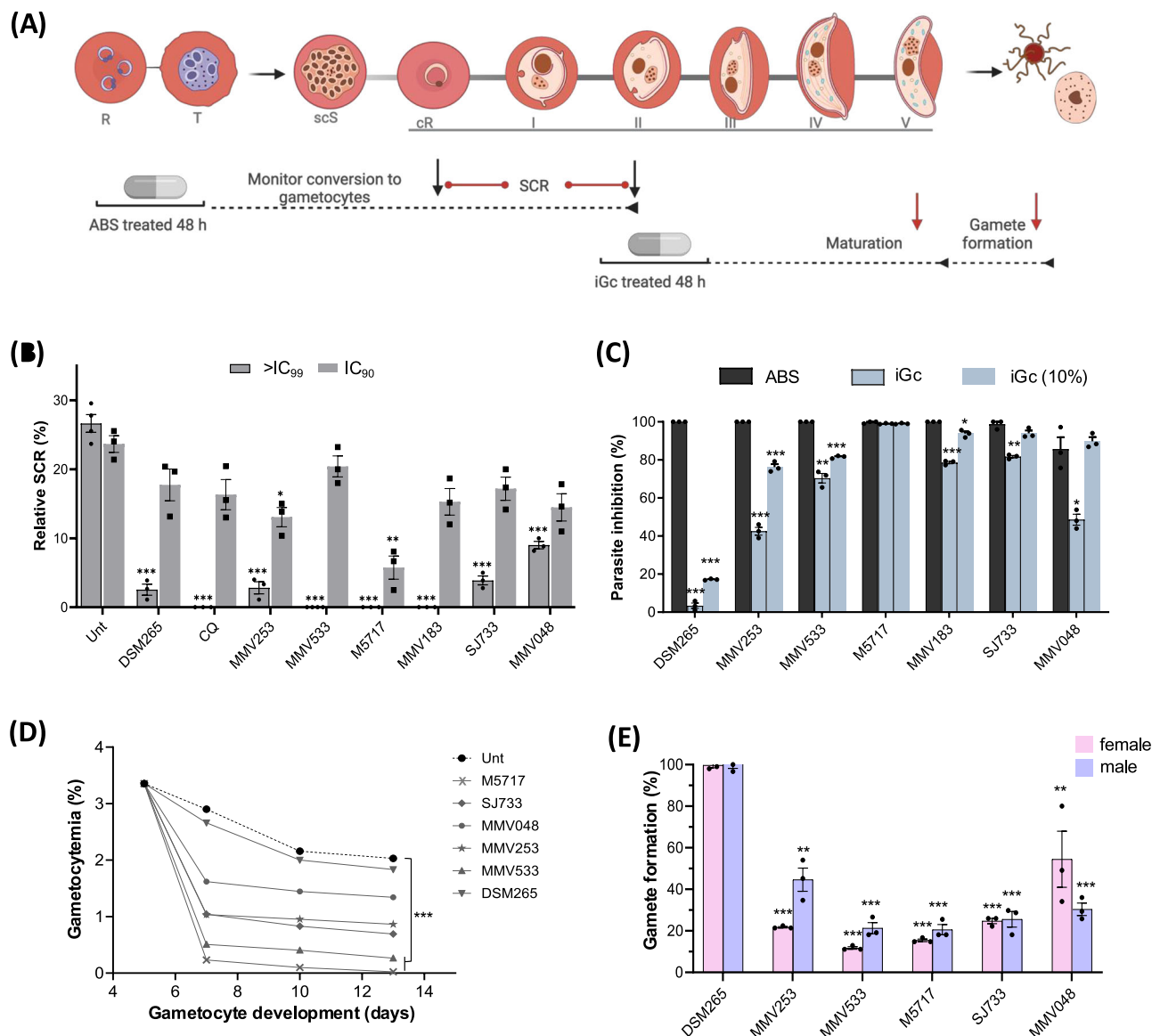


**Fig. 3 | Implications of different inhibition profiles on gametocyte stages.**

**A** Experimental set-up to determine sexual commitment rates (SCR) and gametocyte maturation. Created in BioRender. Birkholtz, L. (2023) [BioRender.com/d75n707](https://www.biorender.com/d75n707). **B** SCR after asexual blood stage (ABS) parasite drug pressure as the ratio of stage II gametocytes on day 4 to ring stages on day 2. Individual data points are indicated in symbols. Data are from three independent biological repeats, in technical triplicates ( $n = 3$ , mean  $\pm$  S.E.). Statistical evaluation was performed with one-way ANOVA (total DF = 26). Exact  $p$ -values are provided in main text.

**C** Inhibition of viability of ABS parasites or immature gametocytes (iGc, >80% stage II/III) as determined with SYBR Green I fluorescence or luciferase expression, respectively. Parasites were exposed to compounds at concentrations corresponding to their therapeutic efficacy in vivo for 48 h for either the same cell numbers between ABS and iGc parasites ( $1 \times 10^5$  cells/well) or reduced iGc numbers

( $1 \times 10^4$  cells/well, 10% iGc). Data are from three independent biological repeats, technical triplicates ( $n = 3$ , mean  $\pm$  S.E.). Individual data points are indicated in symbols. Statistical evaluation was performed with two-way ANOVA (total DF = 62). Exact  $p$ -values provided in Supplementary Data S6. **D** Evaluation of gametocyte maturation after iGc was exposed to compounds for the 48 h period in **C**. Data are from three independent biological repeats ( $n = 3$ ), with one-way ANOVA (total DF = 27) significance evaluation. Exact  $p$ -values provided in main text. **E** The viability of developed mature gametocytes (mGc) was evaluated with male and female gamete formation for three independent biological repeats ( $n = 3$ , mean  $\pm$  S.E.), with technical triplicates. Individual data points are indicated. Statistical evaluation was performed with one-way ANOVA in relation to the untreated control at 100% viability (total DF = 17). Exact  $p$ -values provided in Supplementary Data S6. \* $p < 0.05$ ; \*\* $p < 0.01$ , \*\*\* $p < 0.001$ .

profiles (Fig. 5A). The contribution of tPSA as a discriminator appeared significant to all stages, with lipophilicity (LogP/D) as an important driver to mediate gametocyte activity. This suggests that passive permeability through lipoidal uptake is an essential contributor to compound uptake into various stages of malaria parasites. Since these parameters are typically interrelated, a PCA analysis prioritized the parameters associated with dual activity, with LogD (and LogP) equal drivers of variability in the first dimension (50% of total variability) and tPSA and MW as main contributors in the second dimension (34% of total variability, Fig. 5B). These critical factors suggest the presence of

uptake barriers that prevent compounds from entering mature gametocytes.

### Compound uptake drives inhibition profiles of compounds against ABS parasites and gametocytes

We subsequently validated the contribution of different uptake mechanisms in ABS parasites and gametocytes to explain the differential inhibition profiles of compounds. Parasites take up compounds through lipid diffusion, facilitated uptake through parasite channels or transporter proteins, or new permeability pathways<sup>42</sup> as

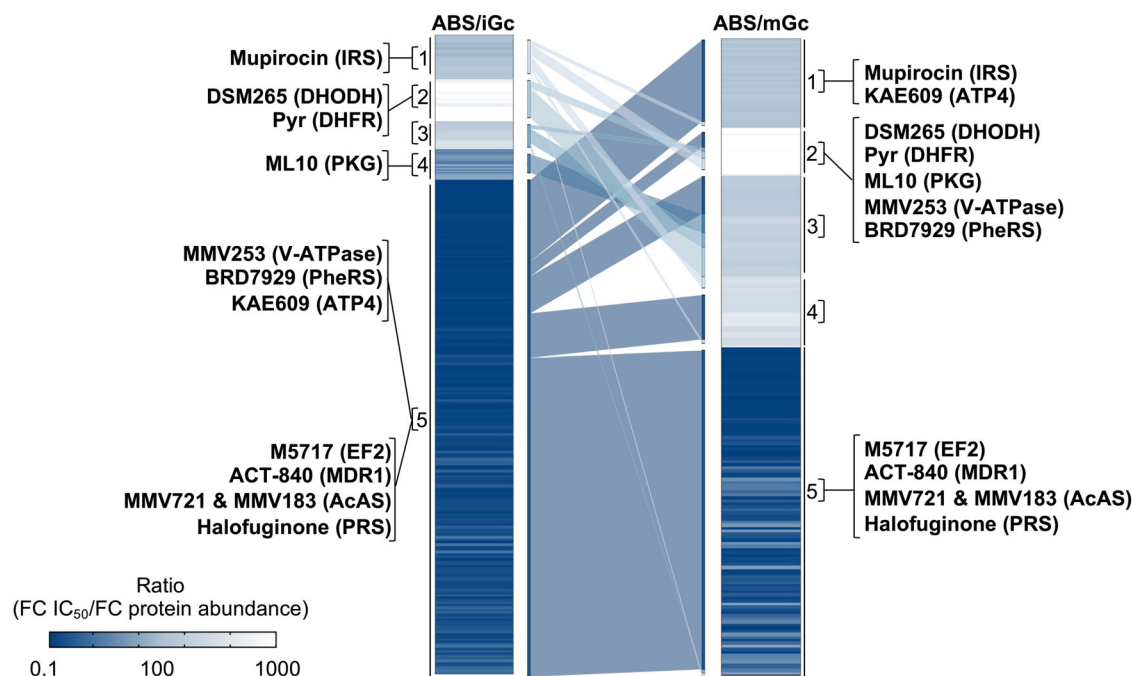


**Fig. 4 | Correlation of abundance of proposed drug targets to compound activities.** The fold change (FC) in a compound's activity ( $IC_{50}$  difference) was calculated as the  $IC_{50}$  ratio measured on asexual blood stage (ABS) parasites vs immature gametocytes (iGc) (ABS/iGc); or ABS parasites vs mature gametocytes (mGc) (ABS/mGc). Additionally, the FC in the protein abundance levels for the drug targets for each compound was calculated for the same parasite stages (FC in protein abundance ABS/iGc or ABS/mGc). The correlation of the amplitude in FC in activity vs the FC in protein abundance was K-means clustered and indicated in the heatmap. The darkest blue indicates compounds nearing a 1:1 ratio between the change in activity of the compound from ABS to i/mGc and the change in that compound's protein abundance. White shows compounds with a considerable loss

in activity but not a similar change in protein abundance. The Sankey diagram between heatmaps illustrates the connection in compounds and their targets between iGc and mGc, as the profile of these compounds changes from active to inactive between these parasite stages. Some compounds and their corresponding targets within each cluster are highlighted. AcAS Acetyl-CoA synthetase, ATP4 non-SERCA-type  $Ca^{2+}$  P-ATPase, DHFR dihydrofolate reductase-thymidylate synthase, DHODH dihydroorotate dehydrogenase, EF2 elongation factor 2, IRS isoleucine-tRNA synthetase, MDR1 multidrug resistance protein 1, PheRS phenylalanine-tRNA synthetase, PKG cGMP-dependent protein kinase, PRS proline-tRNA synthetase, V-ATPase V-type ATPase.

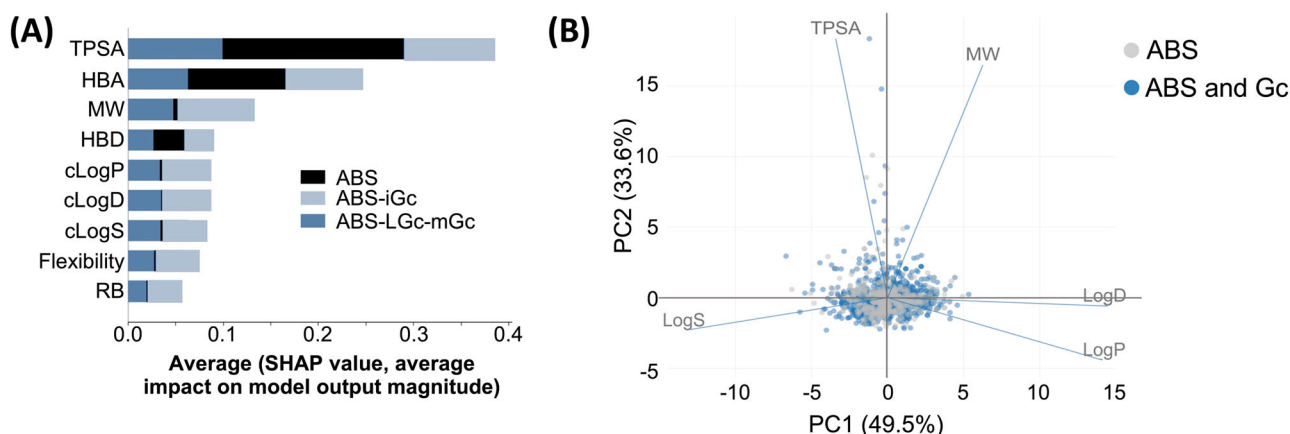


**Fig. 5 | Physicochemical properties of compounds with different activity profiles against ABS parasites and gametocytes.** A Shapely values for the physicochemical properties of the compounds that contributed to the different stage-specific activities. B PCA analysis of the physicochemical properties of compounds

with different activity profiles against asexual blood stage (ABS) parasites and gametocytes. HBA Hydrogen bond acceptor, HBD Hydrogen bond donor, MW Molecular weight, RB Rotatable bonds, tPSA Topological polar surface area.

anion-selective channels (*Plasmodium* surface anion channels, PSAC)<sup>43</sup>. We took advantage of the availability of structurally related analogs of the neutral 2-aminopyridine, MMV048; a basic piperazinylamide containing compound UCT943 and carboxylic acid analog (MMV674594, UCT594) as 2-aminopyrazines (Fig. 6A). These all have PfPI4K as target but display different activity profiles on ABS parasites, immature and mature gametocytes (Fig. 6B)<sup>17,18,44</sup>. UCT943

and UCT594 were designed to improve the solubility and permeability of MMV048, with UCT943 mainly showing decreased lipophilicity. LC-MS detected significantly less of MMV048 and UCT594 inside immature ( $p = 0.049$ ,  $F(2, 6) = 20.15$  and  $p = 0.0003$ ,  $F(2, 6) = 69.57$ , respectively, one-way ANOVA) and late-stage gametocytes ( $p = 0.0018$ ,  $F(2, 6) = 20.15$  and  $p = 0.0001$ ,  $F(2, 6) = 69.57$ , respectively, one-way ANOVA) compared to ABS parasites (Fig. 6C). This

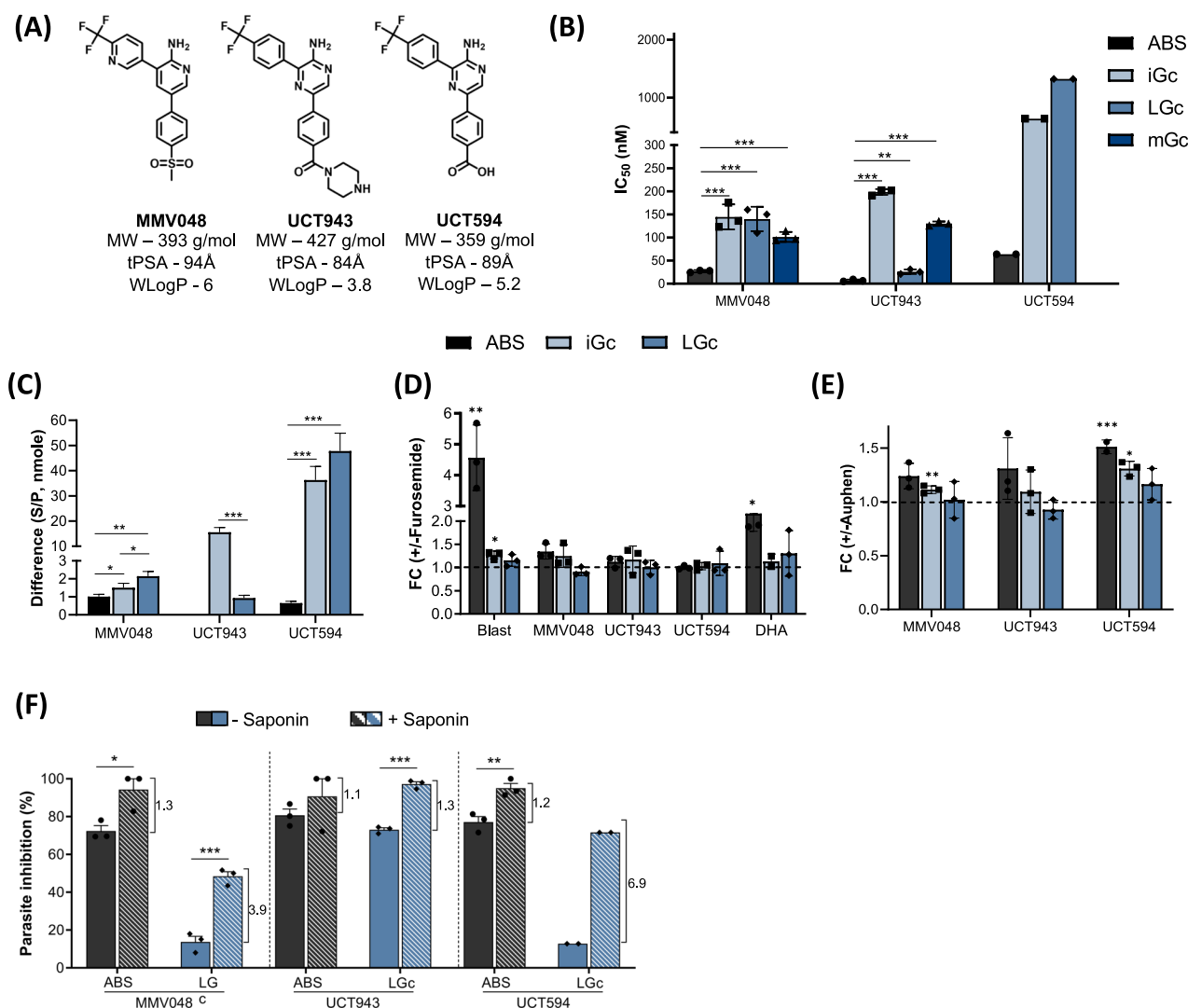


**Fig. 6 | Uptake mechanisms influencing different inhibition profiles of compounds with similar biological targets.** **A** Chemical structures and **B** activities ( $IC_{50}$ ) of MMV048 ( $n = 3$  biological repeats, in triplicate), UCT943 ( $n = 3$ , in triplicate), and UCT594 ( $n = 2$ , published data<sup>17</sup>), mean  $\pm$  S.E. in each instance. Individual data points are indicated in symbols. Statistical evaluation was performed with one-way ANOVA (total DF = 7). Exact  $p$ -values provided in Supplementary Data S6. **C** Difference in the amount of compound present in the supernatant (S) and pellet (P) of asexual blood stage (ABS) parasites and gametocytes (immature (iGc) and late-stage (LGc) gametocytes) as determined with LC-MS ( $n = 1$ , performed in technical triplicates, mean  $\pm$  SD, one-way ANOVA, total DF = 8). Exact  $p$ -values provided in Supplementary Data S6. **D** ABS trophozoites, iGc, and LGc, were either pre-treated with or without Furosemide (PSAC blocker, 30 min) followed by treatment with the positive control (Blasticidin, Blast), MMV048, UCT943, UCT594 and DHA for a further 48 h and proliferation and viability measured with luciferase. Activity is expressed as a fold change (FC) in activity in the presence or absence of Furosemide. Data are from three independent biological repeats, in technical triplicates ( $n = 3$ , mean  $\pm$  S.E.). Individual data points are indicated in symbols.

Statistical evaluation was performed with unpaired two-tailed Student's  $t$  test ( $df = 4$ ). Exact  $p$ -values provided in Supplementary Data S6. **E** ABS parasites, iGc and LGc, were pre-treated with or without Auphen (AQP3 blocker, 30 min), followed by treatment with MMV048, UCT943, and UCT594 for a further 24 h, and proliferation and viability were measured. FC was determined relative to treatments without Auphen. Data are from three independent biological repeats, with technical triplicates ( $n = 3$ , mean  $\pm$  S.E.). Individual data points are indicated in symbols. Statistical evaluation was performed with unpaired two-tailed Student's  $t$  test ( $df = 4$ ). Exact  $p$ -values provided in main text. **F** ABS parasites and LGc were pre-treated with or without saponin (0.05%, 10 min) followed by treatment with MMV048, UCT943, and UCT594 for a further 12 h and viability measured with luciferase, with % inhibition indicated. FC in activity in the presence and absence of saponin are indicated. Data are from three independent biological repeats ( $n = 3$ , mean  $\pm$  S.E.) except for MMV533 in LGc for which data are from  $n = 2$  biological repeats. Individual data points are indicated in symbols. Statistical evaluation was performed with unpaired two-tailed Student's  $t$  test ( $df = 4$ ). Exact  $p$ -values provided in Supplementary Data S6. \* $p < 0.05$ ; \*\* $p < 0.01$ , \*\*\* $p < 0.001$ .

correlates to their activity loss against the gametocyte stages (Fig. 6B). Late-stage gametocytes still took up UCT943, supporting its higher activity against more mature gametocyte stages (Fig. 6C).

Next, we investigated the mechanisms that could contribute to the differential uptake profiles. PSAC increases ABS parasites' permeability and is still active in immature gametocytes but declines as gametocytes mature<sup>11</sup>. Blocking PSAC activity with 30  $\mu$ M Furosemide<sup>45</sup> in ABS trophozoites would decrease the effect of compounds relying on PSAC for entry into the parasites. This treatment decreased

Blasticidin activity 4.5 fold as it is known to be taken up through the PSAC ( $p = 0.0022$ , unpaired Student's  $t$  test, Fig. 6D, Supplementary Fig. S7a, b)<sup>46</sup>. This was also seen for DHA with a 2-fold change in activity ( $p = 0.0144$ , unpaired Student's  $t$  test). However, blocking the PSAC did not have a dramatic influence on the uptake of MMV048, UCT594 or UCT943, with only a 1.3-fold decrease observed in uptake of the neutral MMV048 into ABS trophozoites and immature gametocytes.

Inhibition of aquaglyceroporin (AQP) as a proposed channel for uptake of small molecules into the parasite<sup>47,48</sup>, with the gold(III)



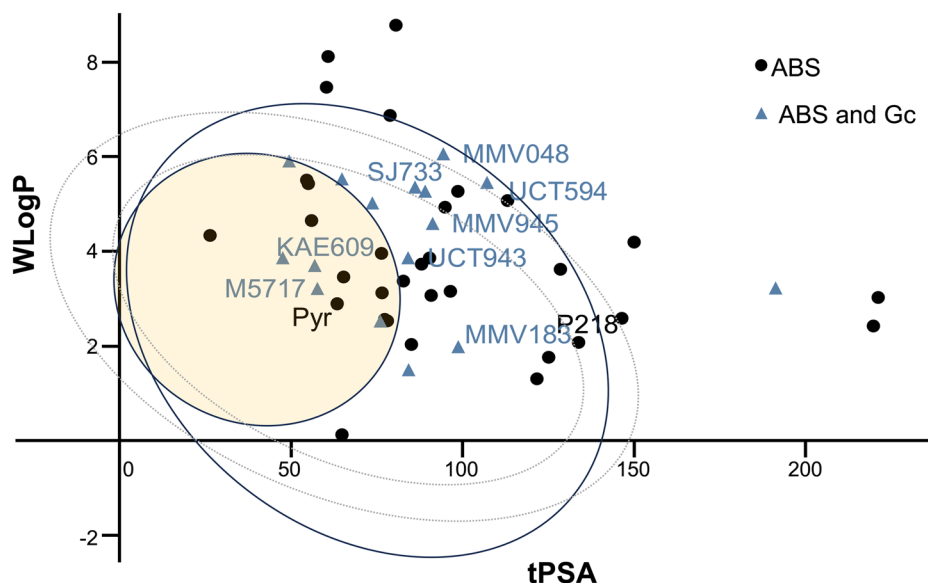


**Fig. 7 | Physicochemical properties of dual-active compounds.** Boiled-egg model (blue ellipses) for frontrunner antimalarials with asexual blood stage (ABS)-specific activity (black) and activity against both ABS parasites and gametocytes (blue). 95%

and 99% confidence ellipses (gray) are shown as indications of good absorption. Pyr Pyrimethamine.

complexed inhibitor Auphen<sup>49</sup> (Supplementary Fig. S7c) resulted in a significant reduction of the activity of MMV048 and UCT594 in ABS parasites ( $p = 0.0001$ , unpaired Student's  $t$  test) and immature ( $p = 0.0089$  and  $p = 0.0312$ , respectively, unpaired Student's  $t$  test) but not mature gametocytes (Fig. 6E, Supplementary Fig. S7d). This indicates some involvement of facilitated uptake via PFAQP of the neutral and acidic compounds into ABS parasites and immature gametocytes but not in mature gametocytes where the abundance of PFAQP is decreased<sup>9,38</sup>, similar to what is observed in *P. berghei* gametocytes compared to ABS parasites<sup>50</sup>.

To investigate the contribution of passive lipid diffusion, the impact of differential lipid compositions was assessed. Late-stage gametocytes treated with saponin, show increased uptake of the membrane-impermeable viability stain TrypanBlue compared to ABS parasites (Supplementary Fig. S7e), as expected given that the mature gametocytes have higher levels of cholesterol<sup>51</sup> resulting in more compact membranes and reduced permeability<sup>52,53</sup>. In the presence of saponin, the activity of the neutral MMV048 and acidic UCT594 dramatically improves 4–7-fold in gametocytes ( $p = 0.0009$  for MMV048, unpaired Student's  $t$  test, Fig. 6F) but not in ABS parasites. The larger, more basic compound UCT943 (Fig. 6F) shows similar activities in both ABS parasites and gametocytes, irrespective of the presence of saponin. Therefore, increased membrane permeability resulted in increased activity of MMV048 and UCT594. The different lipid compositions in ABS parasites compared to gametocytes thus result in reduced diffusion of compounds into gametocytes, which means that dual-active compounds must be designed with specific properties to effectively enter gametocytes via lipid-diffusion mediated uptake.

### Defining the required design parameters for dual-active anti-malarial activity

We subsequently defined the physicochemical space required to ensure dual activity in antimalarial candidates. A Boiled-Egg analysis<sup>54</sup> (Fig. 7) of the predicted lipophilicity (as WLogP from the Wildman-Crippen algorithm related to AlogP<sub>98</sub> but with exhaustive chemical descriptions) *vs* polarity (tPSA) as an indicator of absorption and bioavailability indicated that the majority of frontrunner antimalarials with activity against both ABS parasites and gametocytes fall within the most favorable regions (within the 95% ellipse area). By contrast,

compounds that prefer ABS parasites are also found outside this preferred absorption model. For compounds to have additional activity against gametocytes, these require specific physicochemical properties to support lipid diffusion-mediated uptake which we define here as an optimal tPSA range of 50–75 and WLogP of 3.5–4 (LogD of ~3 preferred), due to the reduced presence of transporters and the unique membrane compositions of gametocytes.

### Discussion

Several frontrunner and development candidates within the anti-malarial portfolio have the additional advantage of targeting the transmission of the parasite from humans to mosquitoes. However, the development pathway of these compounds is centered on their activity against ABS parasites, and the systematic analysis of their effective activity against gametocytes at the concentration needed to kill ABS parasites has not been performed. This limits interpretations as to the consequence of this loss in activity against gametocytes for effective blocking of transmission. Here, we present distinct activity profiles of compounds for ABS parasites and gametocytes associated with specific amplitudes of activity loss and offer causative mechanisms for such profiles.

Our systematic analysis highlighted that the extent of loss of activity of compounds from ABS parasites to mature gametocytes is more pronounced than previously perceived, with even 'equipotent' compounds displaying an average 10- and 18-fold drop in activity against immature and mature gametocytes, which is almost double that which was previously proposed as an expected or acceptable loss<sup>4,10</sup>. We show that this is irrespective of assay platform, exposure time, or parasite strain used, indicative of a persistent phenomenon.

There are several scenarios of concern because of such activity profiles. Compounds without activity against immature gametocytes can cause increased gametocytogenesis due to an escape strategy when ABS parasites are under drug pressure<sup>55</sup>. Although we did not observe this as a systematic issue for the frontrunner compounds we evaluated, we show that gametocytes can still effectively be induced from treated ABS parasites under the conditions tested that mimic therapeutically relevant concentrations. The decreased gametocytocidal capacity of compounds with e.g. an 18-fold drop in activity to mature gametocytes remains a concern. In this scenario, only

compounds (e.g. M5717) with near equipotency between ABS parasites and gametocytes will prevent continuous seeding of the gametocyte population and gametocyte maturation when used at therapeutically relevant concentrations. Only under these circumstances would the gametocyte densities effectively be brought down to less than 1000 gametocytes/mL, the threshold required to prevent sustained transmission of gametocytes<sup>55</sup>. However, increased gametocyte densities have been reported in asymptomatic patients and in pre-elimination, low transmission settings<sup>56,57</sup>, where these parasites switch from replicative to reproductive profiles in response to adaptation to changing environments<sup>57,58</sup>, as has been reported for West African parasite populations<sup>59</sup>. It would be important to model the effective concentration required for gametocytocidal and/or transmission-blocking ability under such conditions. Human dose prediction where the *in vitro* ABS IC<sub>50</sub> is considered (e.g., MMVSola, <https://mmvsola.org/>) could be extended as a model to predict *in vivo* transmission-blocking efficacy at the chosen therapeutic dosages. This would additionally need to take specific pharmacokinetic/pharmacodynamic requirements into account in combinations to allow one partner component to cover the extended 8–12 days for gametocyte maturation<sup>60</sup>.

A critical question that arises is what underlying mechanisms cause these activity profiles. Understanding these factors will provide a framework to guide the design and discovery of the next-generation compounds to ensure successful dual activity. Distinct biological processes are activated to support replication *vs.* reproduction of the parasites, with mature gametocytes metabolically differentiated into a more oxidative state with slower metabolic flux<sup>10,61,62</sup>. We show that the abundance of most drug targets is not predictive of the activity in gametocytes. These targets, not surprisingly, are involved in biological processes of importance to ABS parasites and mature gametocytes, including signaling, translation, and ion homeostasis that all support the mature gametocyte to be in a poised state for onward transmission<sup>10</sup>. However, targeting the same protein between ABS parasites and gametocytes does pose a potential risk. Once resistance develops against these compounds in the ABS parasites, it would spread in the parasite population as gametocytes would not be effectively targeted and, therefore, could continue parasite transmission<sup>2,63</sup>. Characterizing this transmission would contribute to our understanding of the resistance risk of compounds associated with specific drug targets<sup>64</sup>.

A loss in gametocyte activity for some compounds can be attributed to decreased metabolic activities in gametocytes, e.g., CQ and artemisinin derivatives that are dependent on the rate of hemoglobin metabolism in these stages<sup>4</sup>. However, for drugs with specific protein targets indicated, the loss in gametocyte activity did not correlate to reduced target abundance in gametocytes. A lack of data on essentiality, accessibility, subcellular localization, binding affinity, and selectivity of proteins in gametocytes confounds this<sup>55</sup>. Identification and validation of targetable processes crucial to gametocyte survival is therefore required, and genetic manipulation<sup>66,67</sup> or proteomic tools<sup>68,69</sup> have now become available to investigate such processes. Strategies for screening chemical matter *de novo* against transmission stages<sup>69,70</sup> have successfully targeted critical biology in these stages. Our understanding of compounds' transmission-blocking potential would benefit from a systematic model to predict transmission-blocking drug targets and their prioritization.

An important finding of this work is that the loss in activity of compounds against gametocytes correlates to specific requirements in the physicochemical properties to allow for effective diffusion across membranes. The metabolically active trophozoite ABS parasites are enclosed in the intraerythrocytic environment within three associated membrane systems (the erythrocyte membrane, parasitophorous vacuolar membrane, and parasite plasma membrane), with these parasites efficiently inducing additional uptake

mechanisms to overcome this constrain in the form of PSAC<sup>43</sup> and several transport proteins<sup>71</sup>. Gametocytes are also enclosed within three membrane systems together with an additional inner membrane complex (IMC, which is also present in merozoite ABS parasites)<sup>72</sup> that develops under the gametocyte parasite plasma membrane. Uptake mechanisms in gametocytes are limited as the PSAC is absent in mature gametocytes and only a few transport proteins are expressed in these stages<sup>9</sup>. The membrane composition also varies between ABS parasites and gametocytes, with ABS parasites rich in phospholipids required for membrane biogenesis during replication<sup>51,73,74</sup>. By contrast, the membranes of mature gametocytes show increased cholesterol levels (free and esterified)<sup>51</sup>, and sphingolipids<sup>73,74</sup> consistent with increased membrane stability, deformability, and flexibility of mature gametocytes in preparation for transmission<sup>51,75</sup>. We show that these changes pose a significant barrier to drug uptake into the gametocytes, with passive diffusion as the main route of accessibility for compounds. While diffusion and permeability are already critical factors in designing and optimizing lead antimalarial candidates to ensure oral bioavailability<sup>76,77</sup>, this is crucial to ensure added transmission-blocking capabilities with a preference for smaller, neutral, and lipophilic moieties. These are critically important considerations for other infectious organisms, including the *Mycobacterium* bacillus. However, while these characteristics can be used as guiding points in the design of compounds for activity against mature gametocytes, there should be a careful balance towards these additional life cycle profiles compared to an increased propensity towards toxicity and/or metabolic instabilities<sup>78</sup>.

In conclusion, this work provides a framework of activity profiles of antimalarial candidates active against ABS parasites and different stages of gametocytes. We confirm the importance of targeting multiple stages and suggest that activity against immature gametocytes can be a valuable profile to ensure the reduction of the gametocyte load. However, transmission-blocking potential depends on a threshold to provide adequate clearance or, at best, the reduction of mature gametocyte numbers to levels below those that sustain transmission. Next-generation antimalarials could be designed with improved potential for gametocytocidal activity if their targets are similarly expressed between ABS parasites and gametocytes to ensure uptake via diffusion and optimize a compound for transmission-blocking strategies.

## Methods

Extended, comprehensive methods for each section are provided as supplementary material.

## Ethics statement

Parasitology work and volunteer human blood donation (from healthy adult consenting volunteers) at the University of Pretoria is covered under ethical approval from the Research Ethics Committee from Health Sciences (506/2018) and Natural and Agricultural Sciences (180000094).

## In vitro cultivation of *P. falciparum* ABS parasites and gametocytes

*P. falciparum* NF54 (drug-sensitive) ABS parasites were maintained *in vitro* under sterile conditions at 5% hematocrit (A<sup>+</sup>/O<sup>+</sup> human erythrocytes), ~2% parasitemia in complete malaria culture medium (RPMI-1640 supplemented with 23.81 mM NaHCO<sub>3</sub>, 25 mM HEPES, 0.2% (w/v) D-glucose, 0.2 mM hypoxanthine, 0.024 mg/mL gentamicin and 5 g/L Albumax II) under hypoxic conditions (5% O<sub>2</sub>, 5% CO<sub>2</sub> and 90% N<sub>2</sub>) at 37 °C as previously described<sup>7</sup>. In cases where homogeneous ring stages were required, parasites were synchronized with 5% (w/v) D-sorbitol<sup>9</sup>.

As described, immature and mature gametocytes were produced from *P. falciparum* NF54-*pfs16*-GFP-Luc<sup>30</sup> through simultaneous

nutrient starvation and decreased hematocrit<sup>6,7</sup>. ABS cultures (>97% ring-stage parasites, 0.5% parasitemia, 6% hematocrit) were transferred to glucose-deprived complete malaria culture media for 72 h, after which the hematocrit was dropped to 4%. Gametocytogenesis was followed with daily media changes (including glucose) and removal of asexual parasites with 50 mM N-acetylglucosamine from day 1–4 for immature gametocytes (stage II/III) and days 3–7 for late-stage gametocytes (stage IV/V). Gametocytogenesis was monitored daily by microscopy.

### Drug activity assays

SYBR Green I fluorescence was used to determine the activity of compounds (e.g., half-maximal inhibitory concentrations of compounds,  $IC_{50}$ ) against ABS parasites. Ring-stage NF54 *P. falciparum* cultures (1% hematocrit, 1% parasitemia) were treated with compounds (2-fold diluted concentration range from 10  $\mu$ M) for 96 h at 37 °C with chloroquine disulphate (0.5  $\mu$ M) as positive drug control. Fluorescence was measured with 485 nm excitation and 538 nm emission<sup>79</sup>.

The gametocytocidal activity was determined on immature gametocytes (>80% stage II/III), late-stage gametocytes (>90% stage IV/V) or mature gametocytes (>90% stage V) as described using luciferase expression as viability indicator<sup>6</sup> from *P. falciparum* NF54-*pfs16*-GFP-Luc parasites<sup>30</sup>. Activity was determined at 2% gametocytemia, 1.5% hematocrit for 48 h under hypoxic conditions at 37 °C. Methylene blue (5  $\mu$ M) was used as positive control for inhibition. Luciferase activity was measured in 30  $\mu$ L parasite lysates by adding 30  $\mu$ L luciferin substrate (Promega Luciferase Assay System) at room temperature and detecting resultant bioluminescence at an integration constant of 10 s. Assay performance was monitored with Z'-factors at >0.8.

### Generation of constitutively expressed luciferase transgenic line

The site-specific Bxb1 *attB*-*attP* integration system was used to integrate promoter and reporter gene fragments efficiently into the *Plasmodium* genome in the dispensable *cg6* gene of the transgenic NF54-*cg6*-*attB* parasite line (NF54<sup>attB</sup>)<sup>30</sup>. The promoter of nuclear assembly protein (*nap*, PF3D7\_0919000) was identified to regulate constitutive expression across ABS parasites, gametocyte and mosquito stages of *P. falciparum* parasites by examining microarray<sup>9</sup> and RNA sequencing (RNAseq) expression profiles<sup>29</sup>. A myc-tagged CBG99 luciferase fusion gene (click *Pyrophorus plagiophthalmus*)<sup>28</sup> cassette was inserted into *Xho*I and *Not*I sites of pCR2.1-*attP*-FRT-hDHFR/GFP<sup>80</sup> to generate a pCR2.1-*attP*-FRT-hDHFR/GFP-5'*nap*-myc-CBG99-3'*nap* vector where luciferase expression would be under the control of the *nap* promoter once integrated into the genome, confirmed by restriction enzyme mapping and Sanger sequencing. The NF54<sup>attB</sup> line (5–6% ring-stage parasites, 5% hematocrit) was co-transfected with 60  $\mu$ g each of pINT (containing the integrase) and pCR2.1-*attP*-5'*nap*-myc-CBG by electroporation (BioRad Gene Pulser Xcell™ Electroporation System). After 24 h, transgenic parasites were selected with 250  $\mu$ g/mL G418 (neomycin) and 2.5 nM WR99210 for 6 days followed by drug treatment with 2.5 nM WR99210 for an additional 3 days after which parasites recovered in drug-free medium. Genomic integration was confirmed by PCR and sequencing. For wild-type NF54<sup>attB</sup>, the *attB* (B) site was PCR screened with primers F1 (5'-CATCCTGTGAAGTTACCCAGGATCCA-3') and R1 (5'-CATGCAATTCTTGAACCTGTCTATG-3'). For integrated parasites, representing the transgenic line NF54<sup>nap</sup>, the *attL* (L) region was PCR screened with primers F1 (5'-CATCCTGTGAAGTTACCCAGGATCCA-3') and R2 (5'-GATTACTTTGATTAACAAAGGCACGC-3').

Activity of compounds ( $IC_{50}$ ) against NF54<sup>nap</sup> ABS parasites was determined on ring-stage cultures (1% hematocrit, 1% parasitemia) and these parasites were treated with compounds (2-fold diluted concentration range from 10  $\mu$ M) for 96 h at 37 °C with chloroquine disulphate (0.5  $\mu$ M) as positive drug control. The gametocytocidal activity was determined on NF54<sup>nap</sup> immature gametocytes (>80%

stage II/III) or late-stage gametocytes (>80% stage V) at 2% gametocytemia, 1.5% hematocrit for 48 h under hypoxic conditions at 37 °C. Methylene blue (5  $\mu$ M) was used as positive control for inhibition. Luciferase activity in these ABS parasites, immature and late-stage gametocytes produced with this NF54<sup>nap</sup> line (in the presence or absence of compounds) was determined by adding 1 mM non-lysing D-luciferin substrate (0.1M citric acid and 0.1M trisodium citrate 2-hydrate, pH 5.5) at a 1:1 ratio at room temperature<sup>28</sup> and detection of resultant bioluminescence at an integration constant of 10 s.

### Gametocyte commitment rate

For quantification of sexual conversion rates, *Pf*-*efla*-tdTomato parasites were used<sup>34</sup> that express red fluorescence during gametocyte stages. Synchronous ABS parasites (20–26 hpi, 1% parasitemia) were incubated with compounds ( $1 \times IC_{90}$  as determined against ABS parasites) for 48 h at 37 °C. After this, the medium was replaced with drug-free medium daily for an additional 10 days and gametocytogenesis monitored with Giemsa-stained microscopy and fluorescence microscopy, with DAPI (5  $\mu$ g/mL) nuclear co-staining under 1000 $\times$  magnification (Carl Zeiss Axio Lab A1 Fluorescence microscope). Immature gametocyte stages were detected as double-positive fluorescent parasites (parasites positive for both tdTom signal and DAPI-stained nucleic acids) and ABS parasites as DAPI-positive (morphologically confirmed with Giemsa). The sexual conversion rate (SCR) was calculated as the ratio of stage II gametocytes on day four to ring-stage parasites on day two, expressed as a percentage representing gametocyte commitment<sup>7</sup>. Gametocytemia (%) was determined and correlated between Giemsa-staining and fluorescence microscopy.

### Treating immature gametocytes at therapeutically relevant concentrations

Inhibition activities against ABS parasites were determined using SYBR Green I fluorescence assay. Here, ring-stage NF54 *P. falciparum* parasites ( $1 \times 10^5$  parasites/well, 1% hematocrit) were treated with compounds at concentrations mimicking the compounds' therapeutic concentrations, generated either in volunteer infection studies or Phase Ib or IIb clinical trials. ABS parasites were treated at these concentrations for 48 h at 37 °C<sup>79</sup> before measuring fluorescence as above. Additionally, immature gametocytes (>80% stage II/III) were seeded at different cell numbers ( $1 \times 10^5$  gametocytes/well or  $1 \times 10^4$  gametocytes/well). These gametocytes were treated with the compounds at the same concentrations as above for 48 h at 37 °C before luciferase activity was measured as above.

### Drug treatments on immature gametocytes and functional assays

*P. falciparum* immature gametocytes (>80% stage II/III) were seeded in 6-well plates (3.5% gametocytemia) and treated as above for 48 h at 37 °C. Drug was washed out with drug-free media and gametocytemia monitored daily until mature gametocytes were observed (>95% stage V). Male and female gamete formation was evaluated from these mature gametocytes as before<sup>8,81</sup>. Male exflagellating centers were semiautomatically identified for 15 randomly located fields with each video recorded for 8–10 at 30 s intervals and the total exflagellating centers quantified using ICY (open source imaging software GPLv3), normalized to an untreated control<sup>70</sup>. A minimum of 16 centers were counted for the untreated control and methylene blue (10  $\mu$ M) was used as positive control. Female gametes were detected with anti-Pfs25 (FITC labeled) immunofluorescence, counted manually (a minimum of 30 fields counted) at a 100 $\times$  objective using a FITC fluorescence filter, with pyronaridine (10  $\mu$ M) and methylene blue (10  $\mu$ M) as controls<sup>8</sup>.

### Cheminformatic analyses

Biological pathways/protein targets were identified based on text and structure searches for each compound (PubChem [<https://pubchem.ncbi.nlm.nih.gov/>]).



[pubchem.ncbi.nlm.nih.gov/](http://pubchem.ncbi.nlm.nih.gov/)], DrugBank [<https://www.drugbank.ca/>] and the IUPHAR/MMV Guide to Malaria Pharmacology, [[www.guidetomalaria Pharmacology.org/malaria/](http://www.guidetomalaria Pharmacology.org/malaria/)]<sup>82</sup>). Protein expression of selected targets were obtained from published datasets<sup>35,38</sup> for ABS parasites and gametocytes and compared to the compound activities against these stages. Protein abundance values (quantified using the exponentially modified protein abundance index method, emPAI) were compared to the compound activities against these stages. A ratio was calculated between the fold-change in protein abundance and the fold-change in compound activity (as per IC<sub>50</sub> values) between ABS parasites and immature gametocytes, and ABS parasites and mature gametocytes. These ratios were K-means clustered following a within-sum of squares test to determine an optimum number of clusters.

Compound SMILES were extracted for all compounds and their physicochemical properties were predicted using StarDrop (Optibrium, version 7.4) and molecular fingerprints generated (Morgan fingerprints) using RDKit<sup>83</sup>. Activities of compounds against only ABS parasites or against both ABS parasites and gametocytes were predicted from these Morgan fingerprints (500-bit length) using a previously generated model available in Ersilia Model Hub (<https://github.com/ersilia-os/eos80ch>, identifier eos80ch)<sup>40</sup>. These models can only classify compounds as active or inactive against ABS parasites or gametocytes, but cannot differentiate between nuanced activity across multiple stages including immature gametocytes. To overcome this, we built various multiclassification models including random forest (RF) and Gradient Boosting Machines (GBM) using the scikit-learn python package (version 1.2.2)<sup>84</sup>. Due to the imbalanced, multi-class nature of the dataset, oversampling and undersampling techniques (via Imblearn package v 0.10.1) were evaluated but did not improve model performance compared to training on imbalanced data as shown before<sup>40</sup> (Supplementary Data S5). These models were trained on the physicochemical properties of the compounds (predicted with Stardrop v 7.4) as training features within different classes of compounds (classification of compounds based on their original IC<sub>50</sub> values): 1) ABS parasite-specific activity; 2) ABS parasite and immature gametocyte activity; 3) ABS parasite and late/mature gametocyte activity; 4) late/mature gametocyte specific activity. The optimal model is available on Github, <https://github.com/M2PL/Stage-specific-models-for-Pf>. A total of 2013 compounds were randomly split at an 80:20 ratio, whereby 80% of the compounds were used as a training set to train models in classifying compounds to their respective activity profiles based on the compound's predicted physicochemical properties. The resultant 20% was used as a test set to evaluate model performance regarding sensitivity and specificity in classifying specific activity profiles (Supplementary Fig. S6b and Supplementary File S5), from which the top model was identified and further evaluated (RF). A one-*vs*-all ROC curve was generated after a 10-fold cross-validation for each activity profile to determine the RF model's accuracy in predicting individual activity profiles and to assess overall model performance and variance (Supplementary Fig. S6c and Supplementary File S5). To identify critical physicochemical features predictive of a specific activity profile, SHAP values of features were calculated from the model on the training set via Shapely (version 0.44.0)<sup>85</sup>.

For evaluating *in silico* ADME (absorption, distribution, metabolism, and excretion) properties of frontrunner antimalarials with ABS-specific activity and activity against both ABS parasites and gametocytes, SwissADME (<http://www.swissadme.ch/>) and StarDrop were used. Different parameters, including MW, molar refractivity, solubility, gastrointestinal absorption, and bioavailability, were investigated using a radar plot and the BOILED-Egg model to investigate the permeability of frontrunner antimalarials. The BOILED-Egg delineation was predicted, illustrating the capability of gastrointestinal absorption and blood–brain permeation. The BOILED-Egg

model of the antimalarials was created based on their lipophilicity (WLogP) and tPSA. The white elliptical region of the egg depicts high probability of gastrointestinal absorption, while yellow (yolk) round region of the egg depicts blood–brain permeation of compounds<sup>54</sup>. Furthermore, a multivariate approach that defined ranges of LogP and tPSA for well-absorbed and poorly-absorbed compounds<sup>86</sup> was applied on frontrunner antimalarials with differential activity profiles for predicting lipid diffusion mediated uptake of these compounds.

### Validating uptake mechanisms

Uptake of MMV048, UCT943 and UCT594 were performed on *P. falciparum* NF54 trophozoites (>90% trophozoites), immature (>80% stage II/III) and late-stage gametocytes (>90% stage IV/V), at 2% hematocrit and  $1 \times 10^8$  parasites in each suspension. Parasites were treated at  $1 \times \text{IC}_{50}$  for 1 h at 37 °C before the parasites were collected by centrifugation and both the parasite pellets and supernatant samples snap-frozen and stored at –80 °C for LC-MS analysis. Samples were subsequently thawed and extracted with 200  $\mu\text{L}$  ice-cold acetonitrile containing Carbamazepine as internal standard. Calibration standards and quality control samples were prepared by spiking the compounds in the same blank pellet or supernatant matrix to give final concentrations between 3.125 nM and 200 nM. These were also extracted as described and analyzed with the samples to provide a standard curve from which individual concentrations were determined. Analysis was performed on an AB Sciex 4500 Qtrap® mass spectrometer with an electrospray ionization source in positive ionization mode. A Multiple Reaction Monitoring (MRM) method monitored the transitions of the protonated molecular ions to their corresponding daughter ions. The mass spectrometer was coupled to an Agilent 1290 Rapid Resolution HPLC system. Chromatography was achieved using a Poroshell C18 column (30  $\times$  4.6 mm, 2.6  $\mu\text{m}$ ) with 0.1% formic acid as the aqueous mobile phase and 0.1% formic acid in acetonitrile as the organic phase. A gradient method at 0.9 mL/min was run, with a 1:1 split between the MS and waste.

Trophozoites (>90% trophozoites), immature (>80% stage II/III) or late-stage gametocytes (>90% stage IV/V) from *P. falciparum* NF54<sup>nap</sup> line were preincubated with or without either Furosemide (30  $\mu\text{M}$  for 30 min, PSAC/NPP blocker)<sup>45</sup> or Auphen (800 nM for ABS parasites and 5  $\mu\text{M}$  for immature gametocytes and late-stage gametocytes, 30 min, AQP blocker)<sup>49,87</sup>, followed by the addition of  $10 \times \text{IC}_{50}$  of compounds for 6 h at 37 °C. Media was replaced with drug-free medium and incubated for 24 h (Auphen) or 48 h (Furosemide) at 37 °C before luciferase activity was determined as described above. ABS parasites (>90% trophozoites) and late-stage gametocytes (>90% stage IV/V) were also preincubated with or without saponin (0.05% (v/v)) for 10 min at 37 °C, followed by the addition of  $10 \times \text{IC}_{50}$  of compounds for 12 h at 37 °C and viability determined through detecting luciferase activity.

### Data analysis

Unless otherwise specified, all data are presented as the means from at least three independent experiments, each with technical triplicates, with the standard error (S.E.) indicated. All data were tested for normality using the Shapiro–Wilk normality test. Data that were normally distributed were analyzed for statistical significance by unpaired Student's *t* test, one-way ANOVA, or two-way ANOVA, as appropriate. Data that were not normally distributed were analyzed by Kruskal–Wallis non-parametric tests followed by Dunn's multiple comparison test. All statistical tests were evaluated using GraphPad Prism (version 9).

### Reporting summary

Further information on research design is available in the Nature Portfolio Reporting Summary linked to this article.



## Data availability

All data generated or analyzed during this study are included in this published article (and its supplementary information files). Source data are provided with this paper.

## Code availability

All computer codes used to analyze the data are available on GitHub (<https://github.com/M2PL/Stage-specific-models-for-Pf>) and Ersilia (<https://github.com/ersilia-os/eos80ch>; identifier eos80ch).

## References

- World Health Organization. *World Malaria Report 2023* (WHO, 2023).
- Birkholtz, L.-M., Alano, P. & Leroy, D. Transmission-blocking drugs for malaria elimination. *Trends Parasitol.* **38**, 390–403 (2022).
- Josling, G. A. & Llinás, M. Sexual development in *Plasmodium* parasites: knowing when it's time to commit. *Nat. Rev. Microbiol.* **13**, 573–587 (2015).
- Plouffe, D. M. et al. High-throughput assay and discovery of small molecules that interrupt malaria transmission. *Cell Host Microbe* **19**, 114–126 (2016).
- Duffy, S. & Avery, V. M. Identification of inhibitors of *Plasmodium falciparum* gametocyte development. *Malar. J.* **12**, 408 (2013).
- Reader, J., Van Der Watt, M. & Birkholtz, L.-M. Streamlined and robust stage-specific profiling of gametocytocidal compounds against *Plasmodium falciparum*. *Front. Cell. Infect. Microbiol.* **12**, 859 (2022).
- Reader, J. et al. Nowhere to hide: interrogating different metabolic parameters of *Plasmodium falciparum* gametocytes in a transmission-blocking drug discovery pipeline towards malaria elimination. *Malar. J.* **14**, 213 (2015).
- Ruecker, A. et al. A male and female gametocyte functional viability assay to identify biologically relevant malaria transmission-blocking drugs. *Antimicrob. Agents Chemother.* **58**, 7292–7302 (2014).
- Van Biljon, R. et al. Hierarchical transcriptional control regulates *Plasmodium falciparum* sexual differentiation. *BMC Genomics* **20**, 1–16 (2019).
- van der Watt, M. E., Reader, J. & Birkholtz, L.-M. Adapt or Die: Targeting Unique Transmission-Stage Biology for Malaria Elimination. *Front. Cell. Infect. Microbiol.* **12**, 705 (2022).
- Bouyer, G. et al. *Plasmodium falciparum* sexual parasites regulate infected erythrocyte permeability. *Commun. Biol.* **3**, 1–10 (2020).
- Spillman, N. J. et al. Na<sup>+</sup> regulation in the malaria parasite *Plasmodium falciparum* involves the cation ATPase PfATP4 and is a target of the spiroindolone antimalarials. *Cell Host Microbe* **13**, 227–237 (2013).
- Baragaña, B. et al. A novel multiple-stage antimalarial agent that inhibits protein synthesis. *Nature* **522**, 315–320 (2015).
- Kuhen, K. L. et al. KAF156 is an antimalarial clinical candidate with potential for use in prophylaxis, treatment, and prevention of disease transmission. *Antimicrob. Agents Chemother.* **58**, 5060–5067 (2014).
- LaMonte, G. M. et al. Pan-active imidazolopiperazine antimalarials target the *Plasmodium falciparum* intracellular secretory pathway. *Nat. Commun.* **11**, 1–15 (2020).
- McNamara, C. W. et al. Targeting *Plasmodium* PI(4)K to eliminate malaria. *Nature* **504**, 248–253 (2013).
- van der Watt, M. E. et al. Potent *Plasmodium falciparum* gametocytocidal compounds identified by exploring the kinase inhibitor chemical space for dual active antimalarials. *J. Antimicrob. Chemother.* **73**, 1279–1290 (2018).
- Paquet, T. et al. Antimalarial efficacy of MMV390048, an inhibitor of *Plasmodium* phosphatidylinositol 4-kinase. *Sci. Transl. Med.* **9**, ead9735 (2017).
- Phillips, M. A. et al. A long-duration dihydroorotate dehydrogenase inhibitor (DSM265) for prevention and treatment of malaria. *Sci. Transl. Med.* **7**, 296ra111–296ra111 (2015).
- Vanaerschot, M. et al. Inhibition of resistance-refractory *P. falciparum* kinase PKG delivers prophylactic, blood stage, and transmission-blocking antiplasmodial activity. *Cell Chem. Biol.* **27**, 806–816. e808 (2020).
- Baker, D. A. et al. A potent series targeting the malarial cGMP-dependent protein kinase clears infection and blocks transmission. *Nat. Commun.* **8**, 430 (2017).
- Murithi, J. M. et al. The antimalarial MMV688533 provides potential for single-dose cures with a high barrier to *Plasmodium falciparum* parasite resistance. *Sci. Transl. Med.* **13**, eabg6013 (2021).
- Hameed, P. S. et al. Triaminopyrimidine is a fast-killing and long-acting antimalarial clinical candidate. *Nat. Commun.* **6**, 1–11 (2015).
- Taft, B. R. et al. Discovery and preclinical pharmacology of INE963, a potent and fast-acting blood-stage antimalarial with a high barrier to resistance and potential for single-dose cures in uncomplicated malaria. *J. Med. Chem.* **65**, 3798–3813 (2022).
- de Vries, L. E. et al. Preclinical characterization and target validation of the antimalarial pantothienamide MMV693183. *Nat. Commun.* **13**, 1–16 (2022).
- Jiménez-Díaz, M. B. et al. (+)-SJ733, a clinical candidate for malaria that acts through ATP4 to induce rapid host-mediated clearance of *Plasmodium*. *Proc. Natl Acad. Sci.* **111**, E5455–E5462 (2014).
- Le Bihan, A. et al. Characterisation of novel antimalarial compound ACT-451840: preclinical assessment of activity and dose–efficacy modeling. *PLoS Med.* **13**, e1002138 (2016).
- Cevenini, L. et al. Multicolor bioluminescence boosts malaria research: quantitative dual-color assay and single-cell imaging in *Plasmodium falciparum* parasites. *Anal. Chem.* **86**, 8814–8821 (2014).
- López-Barragán, M. J. et al. Directional gene expression and antisense transcripts in sexual and asexual stages of *Plasmodium falciparum*. *BMC Genomics* **12**, 587 (2011).
- Adjalley, S. H. et al. Quantitative assessment of *Plasmodium falciparum* sexual development reveals potent transmission-blocking activity by methylene blue. *Proc. Natl Acad. Sci.* **108**, E1214–E1223 (2011).
- Portugaliza, H. P. et al. Artemisinin exposure at the ring or trophozoite stage impacts *Plasmodium falciparum* sexual conversion differently. *Elife* **9**, e60058 (2020).
- Thommen, B. T. et al. Revisiting the effect of pharmaceuticals on transmission stage formation in the malaria parasite *Plasmodium falciparum*. *Front. Cell. Infect. Microbiol.* **12**, 88 (2022).
- Buckling, A. G., Taylor, L. H., Carlton, J. M. R. & Read, A. F. Adaptive changes in *Plasmodium* transmission strategies following chloroquine chemotherapy. *Proc. R. Soc. Lond. B. Biol. Sci.* **264**, 553–559 (1997).
- McLean, K. J. et al. Generation of transmission-competent human malaria parasites with chromosomally-integrated fluorescent reporters. *Sci. Rep.* **9**, 13131 (2019).
- Lasonder, E. et al. Integrated transcriptomic and proteomic analyses of *P. falciparum* gametocytes: molecular insight into sex-specific processes and translational repression. *Nucleic Acids Res.* **44**, 6087–6101 (2016).
- Bozdech, Z. et al. The transcriptome of the intraerythrocytic developmental cycle of *Plasmodium falciparum*. *PLoS Biol.* **1**, e5 (2003).
- Painter, H. J., Carrasquilla, M. & Llinás, M. Capturing in vivo RNA transcriptional dynamics from the malaria parasite *P. falciparum*. *Genome Res.* **27**, 099549 (2017).
- Silvestrini, F. et al. Protein export marks the early phase of gametocytogenesis of the human malaria parasite *Plasmodium falciparum*. *Mol. Cell. Proteom.* **9**, 1437–1448 (2010).
- Baker, D. A. Malaria gametocytogenesis. *Mol. Biochem. Parasitol.* **172**, 57–65 (2010).
- van Heerden, A., Turon, G., Duran-Frigola, M., Pillay, N. & Birkholtz, L.-M. Machine learning approaches identify chemical features for stage-

- specific antimalarial compounds. *ACS Omega* **8**, 43813–43826 (2023).
41. More, A. & Rana, D. P. in *1st International conference on intelligent systems and information management (ICISIM)*. 72–78 (IEEE, 2017).
  42. Basore, K., Cheng, Y., Kushwaha, A. K., Nguyen, S. T. & Desai, S. A. How do antimalarial drugs reach their intracellular targets? *Front. Pharmacol.* **6**, 91 (2015).
  43. Desai, S. A. Ion and nutrient uptake by malaria parasite-infected erythrocytes. *Cell. Microbiol.* **14**, 1003–1009 (2012).
  44. Brunschwig, C. et al. UCT943, a next-generation *Plasmodium falciparum* PI4K inhibitor preclinical candidate for the treatment of malaria. *Antimicrob. Agents Chemother.* **62**, 00012–00018 (2018).
  45. Kirk, K., Horner, H. A., Elford, B. C., Ellory, J. C. & Newbold, C. I. Transport of diverse substrates into malaria-infected erythrocytes via a pathway showing functional characteristics of a chloride channel. *J. Biol. Chem.* **269**, 3339–3347 (1994).
  46. Hill, D. A. et al. A blasticidin S-resistant *Plasmodium falciparum* mutant with a defective plasmodial surface anion channel. *Proc. Natl Acad. Sci.* **104**, 1063–1068 (2007).
  47. Pavlovic-Djuranovic, S., Kun, J. F., Schultz, J. E. & Beitz, E. Dihydroxyacetone and methylglyoxal as permeants of the *Plasmodium* aquaglyceroporin inhibit parasite proliferation. *Biochim. Biophys. Acta Biomembr.* **1758**, 1012–1017 (2006).
  48. Munday, J. C. et al. *Trypanosoma brucei* aquaglyceroporin 2 is a high-affinity transporter for pentamidine and melaminophenyl arsenic drugs and the main genetic determinant of resistance to these drugs. *J. Antimicrob. Chemother.* **69**, 651–663 (2014).
  49. Martins, A. P. et al. Targeting aquaporin function: potent inhibition of aquaglyceroporin-3 by a gold-based compound. *PLoS One* **7**, e37435 (2012).
  50. Kenthirapalan, S., Waters, A. P., Matuschewski, K. & Kooij, T. W. Flow cytometry-assisted rapid isolation of recombinant *Plasmodium berghei* parasites exemplified by functional analysis of aquaglyceroporin. *Int. J. Parasitol.* **42**, 1185–1192 (2012).
  51. Tran, P. N. et al. Changes in lipid composition during sexual development of the malaria parasite *Plasmodium falciparum*. *Malar. J.* **15**, 73 (2016).
  52. Deng, D., Jiang, N., Hao, S.-J., Sun, H. & Zhang, G.-j. Loss of membrane cholesterol influences lysosomal permeability to potassium ions and protons. *Biochim. Biophys. Acta Biomembr.* **1788**, 470–476 (2009).
  53. Zhang, L. et al. Effect of cholesterol on cellular uptake of cancer drugs pirarubicin and ellipticine. *J. Phys. Chem. B* **120**, 3148–3156 (2016).
  54. Daina, A. & Zoete, V. A boiled-egg to predict gastrointestinal absorption and brain penetration of small molecules. *ChemMedChem* **11**, 1117–1121 (2016).
  55. Collins, K. A. et al. A controlled human malaria infection model enabling evaluation of transmission-blocking interventions. *J. Clin. Invest.* **128**, 1551–1562 (2018).
  56. Bousema, T. & Drakeley, C. Epidemiology and infectivity of *Plasmodium falciparum* and *Plasmodium vivax* gametocytes in relation to malaria control and elimination. *Clin. Microbiol. Rev.* **24**, 377–410 (2011).
  57. Rono, M. K. et al. Adaptation of *Plasmodium falciparum* to its transmission environment. *Nat. Ecol. Evol.* **2**, 377–387 (2018).
  58. Abdi, A. I. et al. *Plasmodium falciparum* adapts its investment into replication versus transmission according to the host environment. *Elife* **12**, e85140 (2023).
  59. Bousema, J. T. et al. *Plasmodium falciparum* gametocyte carriage in asymptomatic children in western Kenya. *Malar. J.* **3**, 1–6 (2004).
  60. Gonçalves, D. & Hunziker, P. Transmission-blocking strategies: the roadmap from laboratory bench to the community. *Malar. J.* **15**, 1–13 (2016).
  61. Ngotho, P. et al. Revisiting gametocyte biology in malaria parasites. *FEMS Microbiol. Rev.* **43**, 401–414 (2019).
  62. Abdel-Haleem, A. M. et al. Functional interrogation of *Plasmodium* genus metabolism identifies species- and stage-specific differences in nutrient essentiality and drug targeting. *PLoS Comp. Biol.* **14**, e1005895 (2018).
  63. Ng, C. L. et al. CRISPR-Cas9-modified *pfmdr1* protects *Plasmodium falciparum* asexual blood stages and gametocytes against a class of piperazine-containing compounds but potentiates artemisinin-based combination therapy partner drugs. *Mol. Microbiol.* **101**, 381–393 (2016).
  64. Duffey, M. et al. Assessing risks of *Plasmodium falciparum* resistance to select next-generation antimalarials. *Trends Parasitol.* **37**, 709–721 (2021).
  65. Forte, B. et al. Prioritization of molecular targets for antimalarial drug discovery. *ACS Infect. Dis.* **7**, 2764–2776 (2021).
  66. Prommana, P. et al. Inducible knockdown of *Plasmodium* gene expression using the glmS ribozyme. *PLoS One* **8**, e73783 (2013).
  67. Tibúrcio, M. et al. A novel tool for the generation of conditional knockouts to study gene function across the *Plasmodium falciparum* life cycle. *mBio* **10**, 01170–01119 (2019).
  68. Bailey, B. L., Nguyen, W., Cowman, A. F. & Sleebbs, B. E. Chemo-proteomics in antimalarial target identification and engagement. *Med. Res. Rev.* **43**, 2303–2351 (2023).
  69. Yahya, S. et al. A novel class of sulphonamides potentially block malaria transmission by targeting a *Plasmodium* vacuole membrane protein. *Dis. Model. Mech.* **16**, dmm049950 (2023).
  70. Reader, J. et al. Multistage and transmission-blocking targeted antimalarials discovered from the open-source MMV Pandemic Response Box. *Nat. Commun.* **12**, 1–15 (2021).
  71. Martin, R. E. The transportome of the malaria parasite. *Biol. Rev.* **95**, 305–332 (2020).
  72. Dearnley, M. K. et al. Origin, composition, organization and function of the inner membrane complex of *Plasmodium falciparum* gametocytes. *J. Cell Sci.* **125**, 2053–2063 (2012).
  73. Gulati, S. et al. Profiling the essential nature of lipid metabolism in asexual blood and gametocyte stages of *Plasmodium falciparum*. *Cell Host Microbe* **18**, 371–381 (2015).
  74. Ridgway, M. C. et al. Analysis of sex-specific lipid metabolism of *Plasmodium falciparum* points to the importance of sphingomyelin for gametocytogenesis. *J. Cell Sci.* **135**, jcs259592 (2022).
  75. Tibúrcio, M. et al. A switch in infected erythrocyte deformability at the maturation and blood circulation of *Plasmodium falciparum* transmission stages. *Blood* **119**, e172–e180 (2012).
  76. Lipinski, C. A., Lombardo, F., Dominy, B. W. & Feeney, P. J. Experimental and computational approaches to estimate solubility and permeability in drug discovery and development settings. *Adv. Drug Del. Rev.* **64**, 4–17 (2012).
  77. Williams, J. et al. Using in vitro ADME data for lead compound selection: An emphasis on PAMPA pH 5 permeability and oral bioavailability. *Bioorg. Med. Chem.* **56**, 116588 (2022).
  78. Gleeson, M. P., Hersey, A., Montanari, D. & Overington, J. Probing the links between in vitro potency, ADMET and physicochemical parameters. *Nat. Rev. Drug Discov.* **10**, 197–208 (2011).
  79. Verlinden, B. K. et al. Discovery of novel alkylated (bis) urea and (bis) thiourea polyamine analogues with potent antimalarial activities. *J. Med. Chem.* **54**, 6624–6633 (2011).
  80. Siciliano, G. et al. A high susceptibility to redox imbalance of the transmissible stages of *Plasmodium falciparum* revealed with a luciferase-based mature gametocyte assay. *Mol. Microbiol.* **104**, 306–318 (2017).
  81. Coetzee, N. et al. Epigenetic inhibitors target multiple stages of *Plasmodium falciparum* parasites. *Sci. Rep.* **10**, 1–11 (2020).
  82. Armstrong, J. F. et al. Advances in Malaria Pharmacology and the online Guide to MALARIA PHARMACOLOGY: IUPHAR Review X. *Br. J. Pharmacol.* **180**, 1899–1929 (2023).

83. Landrum, G. *RDKit: Open-source cheminformatics*, <https://www.rdkit.org/> (2006).
84. Pedregosa, F. et al. Scikit-learn: Machine learning in Python. *J. Mach. Learn. Res.* **12**, 2825–2830 (2011).
85. Lundberg, S. M. & Lee, S.-I. A unified approach to interpreting model predictions. *Adv. Neural Inf. Process. Syst.* **30**, <https://doi.org/10.48550/arXiv.1705.07874> (2017).
86. Egan, W. J., Merz, K. M. & Baldwin, J. J. Prediction of drug absorption using multivariate statistics. *J. Med. Chem.* **43**, 3867–3877 (2000).
87. Posfai, D. et al. *Plasmodium* parasite exploits host aquaporin-3 during liver stage malaria infection. *PLoS Path.* **14**, e1007057 (2018).

## Acknowledgements

We thank Banothile Makhubela from the University of Johannesburg for Auphen. This project was in part supported by the Medicines for Malaria Venture (L.M.B.: RD-19-001). South African Medical Research Council and the Department of Science and Innovation South African Research Chairs Initiative Grants managed by the National Research Foundation (L.M.B. UID: 84627). The University of Pretoria Institute for Sustainable Malaria Control acknowledges the South African Medical Research Council as Collaborating Centre for Malaria Research. K.C. is the Neville Isdell Chair in African-centric Drug Discovery and Development and thanks Neville Isdell for generously funding the Chair.

## Author contributions

M.N. performed the work with J.R. including data analyses with A.v.H. and M.v.d.W. D.J. and G.S., with P.A. assisted with the line generation. M.Njoroge assisted with the uptake experiments under K.C. with J.N. assisting with interpretations. L.M.B. conceptualized and supervised the study with E.H. and D.L. and wrote the paper with M.N. All co-authors approved the final version of the manuscript.

## Competing interests

D.L. is a senior director in drug discovery at the Medicines for Malaria Venture (M.M.V.). M.M.V. funded part of this study. The other authors declare no competing interest.

## Additional information

**Supplementary information** The online version contains supplementary material available at <https://doi.org/10.1038/s41467-024-54144-x>.

**Correspondence** and requests for materials should be addressed to Lyn-Marié. Birkholtz.

**Peer review information** *Nature Communications* thanks Nikhil Pillai and the other, anonymous, reviewer(s) for their contribution to the peer review of this work. A peer review file is available.

**Reprints and permissions information** is available at <http://www.nature.com/reprints>

**Publisher's note** Springer Nature remains neutral with regard to jurisdictional claims in published maps and institutional affiliations.

**Open Access** This article is licensed under a Creative Commons Attribution-NonCommercial-NoDerivatives 4.0 International License, which permits any non-commercial use, sharing, distribution and reproduction in any medium or format, as long as you give appropriate credit to the original author(s) and the source, provide a link to the Creative Commons licence, and indicate if you modified the licensed material. You do not have permission under this licence to share adapted material derived from this article or parts of it. The images or other third party material in this article are included in the article's Creative Commons licence, unless indicated otherwise in a credit line to the material. If material is not included in the article's Creative Commons licence and your intended use is not permitted by statutory regulation or exceeds the permitted use, you will need to obtain permission directly from the copyright holder. To view a copy of this licence, visit <http://creativecommons.org/licenses/by-nc-nd/4.0/>.

© The Author(s) 2024